

**STABILIZED MODE-LOCKING OF THE
FIGURE EIGHT LASER**

By

V. V. PRASAD DASIKA

Bachelor of Engineering

Visveswaraya Institute of Technology

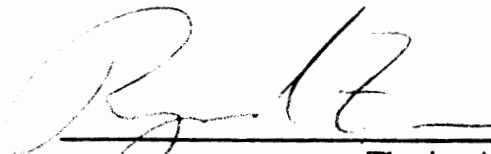
Bangalore, India

1991

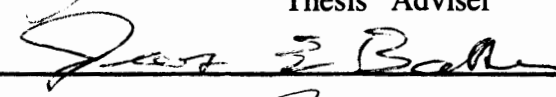
**Submitted to the Faculty of the
Graduate College of the
Oklahoma State University
in partial fulfillment of
the requirements for
the Degree of
MASTER OF SCIENCE
December, 1993**

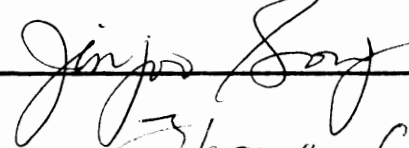
STABILIZED MODE-LOCKING OF THE
FIGURE EIGHT LASER


Thesis Approved :



Thesis Adviser







Dean of the Graduate College

PREFACE

In this study I have attempted to demonstrate the principle of operation of the Figure Eight Laser with the goal of using this laser in future communication systems.

I have tried at every possible stage to present my understanding of the phenomena in the simplest possible terms. With great respect to the brevity of mathematics I have tried to limit its usage at the risk of becoming verbose.

I would like to thank Dr. Raymond Zanoni for serving as my adviser during this work. I am deeply indebted to him for the constant encouragement and unflinching support he has provided me. I am also grateful to the Oklahoma Committee for the Advancement of Science and Technology (OCAST), Frontier Engineering Inc., and Williams Telecommunications Inc., for supporting this work. I would also like to thank Dr. Jin-Joo Song and Dr. James Baker for agreeing to serve on my committee. I also wish to thank my friend, guide and philosopher, Dr. Vladimir Pelekhaty, Research Scientist at the Center for Laser Research, for his untiring efforts and invaluable encouragement. Dr. Pelekhaty has been instrumental in discovering the origin of instability in the Figure Eight Laser. As a comrade he has reinforced my belief that it is the quest for perfection that validates human existence.

TABLE OF CONTENTS

Chapter		Page
I.	INTRODUCTION.	1
II.	THEORY OF FIGURE EIGHT LASER.	5
	Nonlinear Optical Loop Mirror	5
	Polarization Consideration	16
	Nonlinear Amplifying Loop Mirror.	20
III.	ERBIUM DOPED FIBER AMPLIFIERS.	31
	Mode-locking	48
	Gain Switching.	49
	Q-Switching.	50
	Mode-locking.	50
IV.	EXPERIMENTAL INVESTIGATIONS.	57
	Characterization of Erbium Doped Fiber Amplifiers.	57
	Measurement of Decay Constants	58
	Measurement of Threshold Pump Power.	64
	Figure Eight Laser.	68
	Polarization Controllers	68
	Isolator	72
	Figure Eight Laser	74
V.	INSTABILITY	81
VI.	SUMMARY AND CONCLUSIONS.	91

LIST OF FIGURES

Figure	Page
1. Sagnac Interferometer.	6
2. Anti-Resonant Ring Cavity	8
3. Schematic of the Nonlinear Optical Loop Mirror	11
4. Transfer Function of the Nonlinear Optical Loop Mirror for Couplers with Splitting Ratio of 90 : 10 & 60 : 40	15
5. Propagation of Instantaneous Field Vector Around the Loop.	17
6. Schematic of the Nonlinear Amplifying Loop Mirror.	21
7. Transmission & Reflection Characteristic of the Nonlinear Amplifying Loop Mirror.	26
8. Transmitted and Reflected Output of NALM.	28
9. Illustration of Pump ESA.	36
10. Normalized Length vs Normalized Output Power	39
11. Normalized Gain vs Normalized Pump Power	40
12. Normalized Gain vs Normalized Length.	42
13. Plot Showing Optimum Gain and Optimum Pump for Normalized Fiber Lengths	43
14. Normalized Signal Output Power vs Normalized Pump Power.	44
15. Normalized Signal Input/Output Power Characteristics	45
16. Normalized Gain vs Normalized Length for Saturated Regime.	47

Figure	Page
17. Schematic of the Experimental Setup Used for Measurements	59
18. Schematic of the Sliding Detector	61
19. Normalized Length vs Normalized Pump Power	63
20. Pump Decay	65
21. Signal Decay	66
22. Schematic of the Figure Eight Laser.	69
23. Pulses Recorded by the Detector.	76
24. Spectrum of the Pulses.	77
25. Low Frequency Modulation.	78
26. Structure of Low Frequency Modulation.	79
27. Timing Diagram.	82
28. Schematic of the Modified Figure Eight Laser.	86
29. Spectrum of the Pulses	87
30. Pulses Recorded by the Detector	88
31. Autocorrelation of the Output Pulses.	89

CHAPTER I

INTRODUCTION

The technological advancement that has occurred in the Twentieth century is unparalleled in the history of mankind. With the development of technology, the need to transfer information has grown. As the world shrinks under the technological development, one concept that has made fast data transfer possible is the development of optical communications. As communication companies are trying to gear up to meet the demands of posterity, scientists around the world are working on devices that will make faster data transfer possible and reliable. With the realization of the advantages, of speed, of all-optical switching there is a renewed thrust to develop such devices. As the much talked about soliton communications come closer to reality, the search for soliton sources has intensified. In this context the need for the development of fiber lasers assumes paramount importance. Fiber lasers are an attractive proposition for communication systems because they consume less power, are compact and are inexpensive to build and use. The Figure Eight Laser is, but a step towards developing compact pulsed femtosecond lasers. The Figure Eight Laser, apart from being a passively mode-locked laser, also incorporates an all-optical switch, therefore time invested in the study of this all-fiber pulse generator is bound

to pay rich dividends in the form of pushing the frontiers of technology.

In January 1988, Doran and Wood¹ with the British Telecom Research Laboratories reported the development of the Nonlinear Optical Loop Mirror. It can be described as a saturable reflector. But the intensities required to saturate the device were high. In August 1989 Mohammed Islam et. al² reported soliton switching in the nonlinear loop mirror. Two years later in the summer of 1990, Fermann et. al³ reported the development of the Nonlinear Amplifying Loop Mirror, an improvement over the Nonlinear Optical Loop Mirror. Since then the nonlinear loop has been a subject of great interest because of its all optical switching capability. The addition of an amplifier as devised by Fermann has heightened the interest in this device as a highly efficient switching scheme. A year later Duling III⁴ reported the development of a mode-locking scheme incorporating the Nonlinear Amplifying Loop Mirror and called it the Figure Eight Laser. His experiments attracted worldwide interest because of the ability of the configuration to produce solitons. Since then D. J. Richardson and his group at the University of Southampton has conducted numerous studies^{5,6} on this device.

In early 1992 Yoshida et. al⁷ announced their method to control the repetition rate of the laser. But one question that has troubled everyone who has worked with this laser is, what seemed to be its inherent, instability. The instability of mode-locking or intermittent pulsing or the inequitable distribution of energy across the gain bandwidth of the Erbium Doped Fiber Amplifier. It was speculated that the source of instability was the polarization dependent switching properties of the nonlinear loop⁸.

In an effort to understand the operation of this laser, I started in chronological order and over time constructed the Figure Eight Laser. This offered a comprehensive view of the problems involved in the laser. In this work, I present the hypothesis of gain modulation in the Erbium Doped Fiber Amplifier that accounts for the instabilities observed.

The work has essentially been divided into two categories, theoretical and experimental. Chapter II presents the theoretical background and simulation of the nonlinear loops. Chapter III begins with an introduction to the Erbium Doped Fiber Amplifiers leading to the principles of mode-locking. Chapter IV presents the experimental investigations along with the results obtained. It also discusses the principle of operation and method of fabrication of the various devices used to make the Figure Eight Laser. Chapter V presents the problem of instability. A thorough analysis of the results obtained during the experiments culminates with the solution to the problem of instability.

In consonance with Thomas Hardy's statement, "The petty done, the undone vast," I conclude the discussion with the scope for future research in Chapter VI.

FOOTNOTES

¹N. J. Doran and David Wood, *Opt. Lett.* 13, 56 (1988).

²M. N. Islam, E. R. Sunderman, R. H. Stolen, W. Pleibel and J. R. Simpson, *Opt. Lett.* 15, 811 (1989).

³M. E. Fermann, F. Habrel, M. Hofer and H. Hochreiter, *Opt. Lett.* 15, 752 (1990).

⁴Irl N. Duling III, *Opt. Lett.* 16, 539 (1991).

⁵D. J. Richardson, V. V. Afanasjev, A. B. Grudinin and D. N. Payne, *Opt. Lett.* 17, 1596 (1992).

⁶D. J. Richardson, R. I. Laming, D. N. Payne, M. W. Phillips, V. J. Mastas, *Elect. Lett.* 27, 730 (1991).

⁷Eiji Yoshida, Yasuo Kimura and Masataka Nakazawa, *Appl. Phys. Lett.* 60, 932 (1992).

⁸N. Finlayson, B. K. Nayar and N. J. Doran, *Opt. Lett.* 17, 112 (1992).

CHAPTER II

THEORY OF THE FIGURE EIGHT LASER

The aim of this chapter is to obtain a thorough understanding of the device configurations that have led to the development of the Figure Eight Laser (F8L). To this end I begin the discussion with the simple Sagnac interferometer and a discussion on the importance of asymmetry in the configuration leading to a discussion of the Nonlinear Optical Loop Mirror (NOLM). With a thorough understanding of the NOLM we study the operation of the Nonlinear Amplifying Loop Mirror (NALM). Finally, polarization and dispersion effects are considered.

Nonlinear Optical Loop Mirror

A schematic of the Sagnac interferometer² is shown in Figure 1. Light from the source is split into two beams that travel in the clockwise and counter-clockwise direction to reach the beamsplitter. Depending on the differential phase shift the amount of light incident on the detector changes. Let us consider the operation of the Sagnac interferometer in detail. Light from the source is split into two beams by

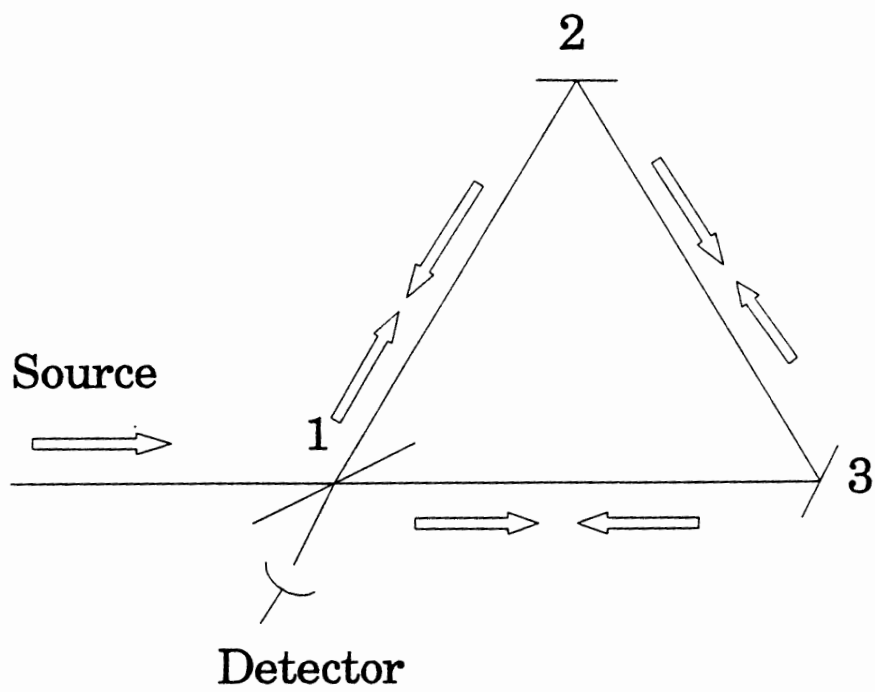


Figure 1. Sagnac Interferometer

the beamsplitter. The clockwise propagating beam after reflection from mirrors 1 and 2 reaches the beamsplitter. The counter-clockwise propagating beam after reflection from mirrors 2 and 1 reaches the beamsplitter. These two beams then interfere leading to variation in the amount of light detected depending on the phase shift. In the schematic shown (Refer Fig. 1) the optical path lengths traversed by the two beams are identical. The main feature of this device is that the two identical but oppositely directed paths taken by the beams form a closed loop before being united to produce interference. This device can also be looked at in the light of Stokes relations³. Figure 2 shows the schematic of the anti-resonant ring cavity. According to Stokes relations

$$r = -r' \quad (2-1a)$$

$$r^2 + t t' = 1 \quad (2-1b)$$

where r , r' , t and t' are the amplitude reflection and transmission coefficients as illustrated in Figure 2. Let the incident field be E_0 . Let us consider the two counter propagating beams separately.

$$E_{(t, cw)} = E_0 t^2 \quad (2-2a)$$

$$E_{(t, ccw)} = E_0 r r' \quad (2-2b)$$

where cw and ccw represent the clockwise and counter-clockwise propagating components. Then, the total field is equal to the sum of the clockwise and counter-clockwise propagating signals.

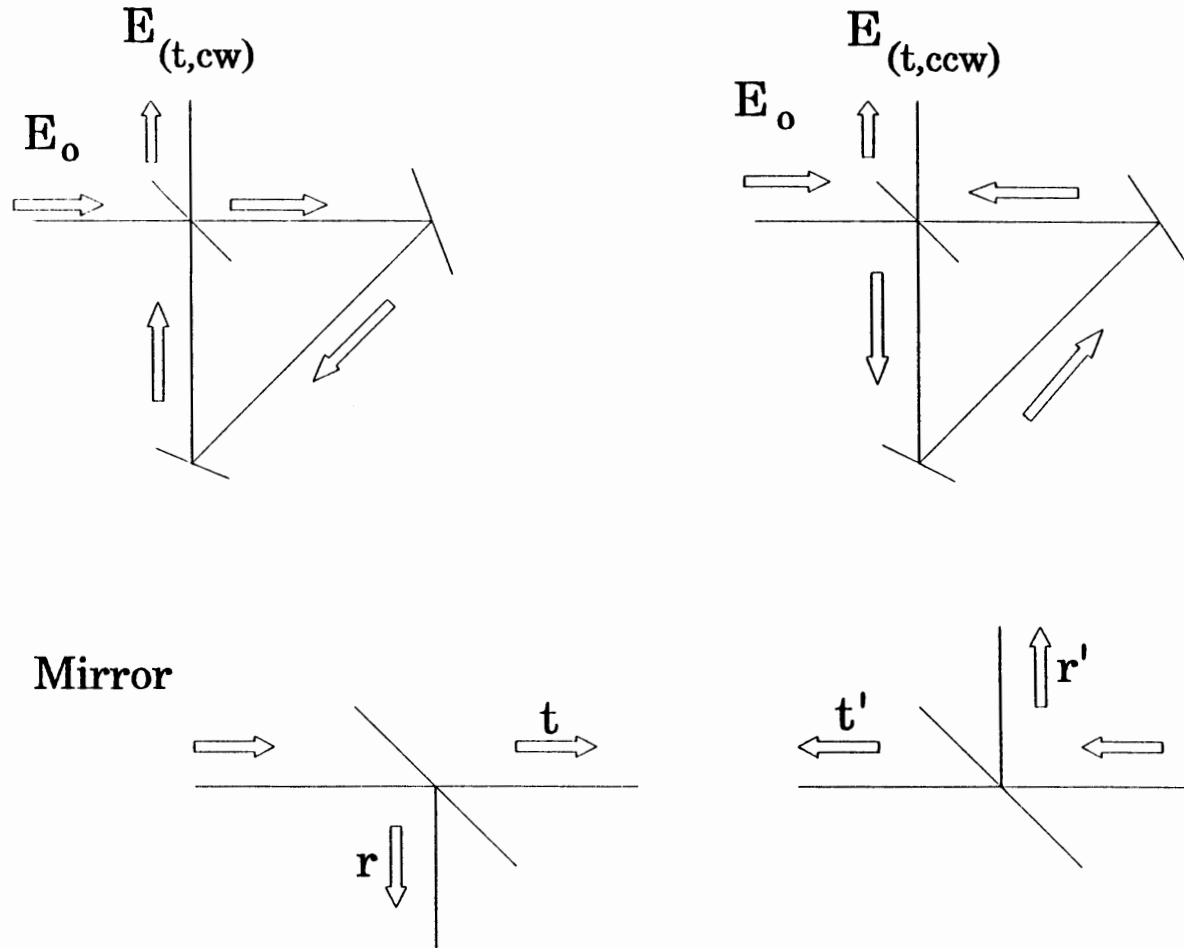


Figure 2. Anti-Resonant Ring Cavity

Therefore

$$E_{(t, cw)} + E_{(t, ccw)} = E_o (t^2 + r r') \quad (2-3)$$

this shows that the total field is equal to zero if (using Stokes relations Eqns (2-1a) and (2-1b))

$$r = t \quad (2-4)$$

This is applicable to mirrors, beamsplitters and directional couplers provided there is no absorption. The Sagnac interferometer has been used as a gyroscope to measure the rotation rate of a system. The idea is that when the whole setup is rotated about an axis perpendicular to the axis passing through the center, the beam travelling in the direction of rotation travels an effective distance that is less than the distance travelled by the beam travelling in the opposite direction. The difference in the distance travelled manifests itself as the phase shift resulting in light being switched out. This is one of the methods used to introduce asymmetry in the Sagnac interferometer to facilitate the accumulation of differential phase shift. Another method of obtaining the same effect is placing an optical amplifier asymmetrically and propagating the beam in a nonlinear medium wherein the refractive index encountered by the signal is proportional to the intensity. The difference in the refractive index encountered will result in differential phase shift between the two beams leading to interference. Since switching depends on the phase shift that is introduced, it is important to be able to identify ways to achieve the same without infringing on the stability of the system.

As stated earlier the NOLM¹ is the forerunner of the NALM⁴ which is the

basis for the F8L⁵. A schematic of the NOLM is shown in Figure 3. It is fabricated by splicing two legs of a directional coupler with unequal splitting ratio. The advantage of this device is that it does not require interferometric alignment although it is an interferometer. It is robust and is of simple construction. This device operates in two regimes, linear and nonlinear. But, before launching into a discussion of the operating regimes, it is important to build a bridge between the Sagnac loop and the NOLM. Consider the schematic shown in Figure 3 with a coupler splitting ratio of 50 : 50. Two beams originate in the NOLM: one travelling clockwise and the other counter-clockwise. Since there is no difference in the path lengths encountered by the two counter propagating beams, no differential phase shift accumulates, and when the two beams re-enter the coupler, they interfere constructively leading to all light being reflected by the device. This is similar in operation to the Sagnac loop discussed earlier.

Now consider a NOLM made using a directional coupler with an unequal splitting ratio. Let us examine the operation of this device in the linear and the nonlinear regimes. The device is said to be operating in the linear regime if the input powers are low enough so as not to cause any perceptible intensity dependent behavior. The device enters the nonlinear regime of operation at very high input powers, i.e. at powers where self-phase modulation plays an important role in the reflection and transmission properties of the NOLM.

The linear regime of operation is considered first. Light coupled into port 1 is split into two signals of unequal intensities by the coupler. Light in port 3 of the

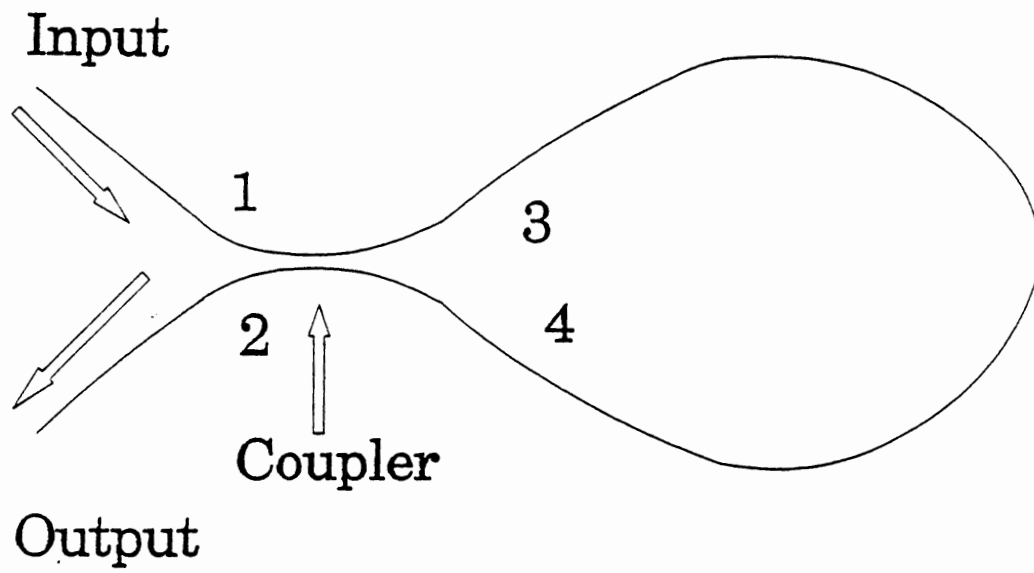


Figure 3. Schematic of the Nonlinear Optical Loop Mirror

coupler travels clockwise towards port 4, whereas light in port 4 of the coupler travels counter-clockwise towards port 3. Thus there are two counter propagating beams travelling in the loop. This is the setup of a typical Sagnac interferometer. Even though the splitting ratio of the coupler is unequal, the two counter propagating beams traverse the same optical path length, as the intensity of the input signal is low. Since both the signals traverse the same distance, there is no differential phase shift. When the two beams re-enter the coupler after travelling the loop of length L , they interfere constructively in the coupler and light is reflected back to port 1. It is assumed that the polarization is preserved along the length of the loop. This can be done by using a polarization preserving fiber to make the loop⁶. Polarization changes in the input signal will be considered later. This is the linear mode of operation of the loop. The linear mode of operation is characterized by the behavior of the loop as a reflector (excluding the transmission losses in the fiber and insertion loss of the coupler) when polarization is preserved as the signal traverses the loop.

The NOLM enters the nonlinear mode of operation when the input signal is of very high intensity. Typical electric field intensity required to see such nonlinear effects is of the order of hundreds of KW / m^2 . Pulses of such high intensity are usually obtained using a mode-locked laser. Signal coupled into port 1 is split into two signals of unequal intensity. Let the splitting ratio of the directional coupler be $\alpha : 1 - \alpha$. When $\alpha \neq 0.5$, the two counter propagating signals in the loop are of different intensities. Since the signal is of very high intensity, the total optical path length encountered by the two counter propagating signals is different. This is

because of the intensity dependence of refractive index according to $n_0 + n_2 I$, where I is the intensity of the relatively intense signal. Since the refractive index encountered by the signals is different, there accumulates a differential phase shift between the two counter propagating signals. Let the phase change for the clockwise and counter-clockwise propagating beams be $\delta\phi_c^{NL}$ and $\delta\phi_{cc}^{NL}$ respectively. Then

$$\delta\phi_c^{NL} = \frac{\pi}{\lambda} n_2 I \alpha L \quad (2-5a)$$

$$\delta\phi_{cc}^{NL} = \frac{\pi}{\lambda} n_2 I (1 - \alpha) L \quad (2-5b)$$

From the above equations, the differential phase shift is calculated to be

$$\Delta\phi = \frac{\pi}{\lambda} n_2 I L (1 - 2\alpha) \quad (2-6)$$

It is seen that the phase shift suffered by a signal is a function of the coupler splitting ratio. If $\alpha = 0.5$ there is no differential phase shift between the two signals, therefore the signals will interfere constructively and all the power is reflected back to port 1. When $\alpha \neq 0.5$, differential phase shift plays an important role and depending on the magnitude of the differential phase shift signal, is either partially reflected and partially transmitted or completely transmitted through port 2. It is seen that the intensity required to obtain complete switching is

$$I_\pi = \frac{\lambda}{n_2 L (1 - 2\alpha)} \quad (2-7)$$

The equations governing the input and output fields for a coupler with a power-

coupling ratio $\alpha : 1 - \alpha$ are

$$E_3 = \alpha^{1/2} E_1 + i(1 - \alpha)^{1/2} E_2 \quad (2-8a)$$

$$E_4 = i(1 - \alpha)^{1/2} E_1 + \alpha^{1/2} E_2 \quad (2-8b)$$

As the fields travel around the loop length L the fields E_3 , E_4 are given by

$$E_3 = \sqrt{\alpha} E_i e^{i\alpha |E_i|^2 \frac{L}{2\lambda} n_2 n_0 c} \quad (2-9a)$$

$$E_4 = (1 - \alpha)^{1/2} E_i e^{i(1-\alpha) |E_i|^2 n_2 n_0 \frac{c}{\lambda}} \quad (2-9b)$$

Substituting Eqn (2-9a) and (2-9b) in the Eqn (2-8a), we obtain

$$|E_{02}|^2 = |E_i|^2 (1 - 2\alpha(1 - \alpha) [1 + \cos[(1 - 2\alpha) |E_i|^2 n_0 n_2 \frac{c}{2\lambda}]]) \quad (2-10)$$

This equation shows that for any value of $\alpha \neq 1$, 100% of the power emerges from port 2 provided:

$$n_2 n_0 c |E_i|^2 L / 2\lambda = m(\pi / (1 - 2\alpha)) \quad (2-11)$$

for odd m . The minimum power occurs for even m given by

$$|E_{02}|^2 = |E_i|^2 [1 - 4\alpha(1 - \alpha)] \quad (2-12)$$

Figure 4 shows the transfer function at port 2 as a function of input power and length for two values of α (0.1 and 0.4). It is seen that the best switching contrast occurs for α closest to 0.5. It should be noted that any interaction between the counter

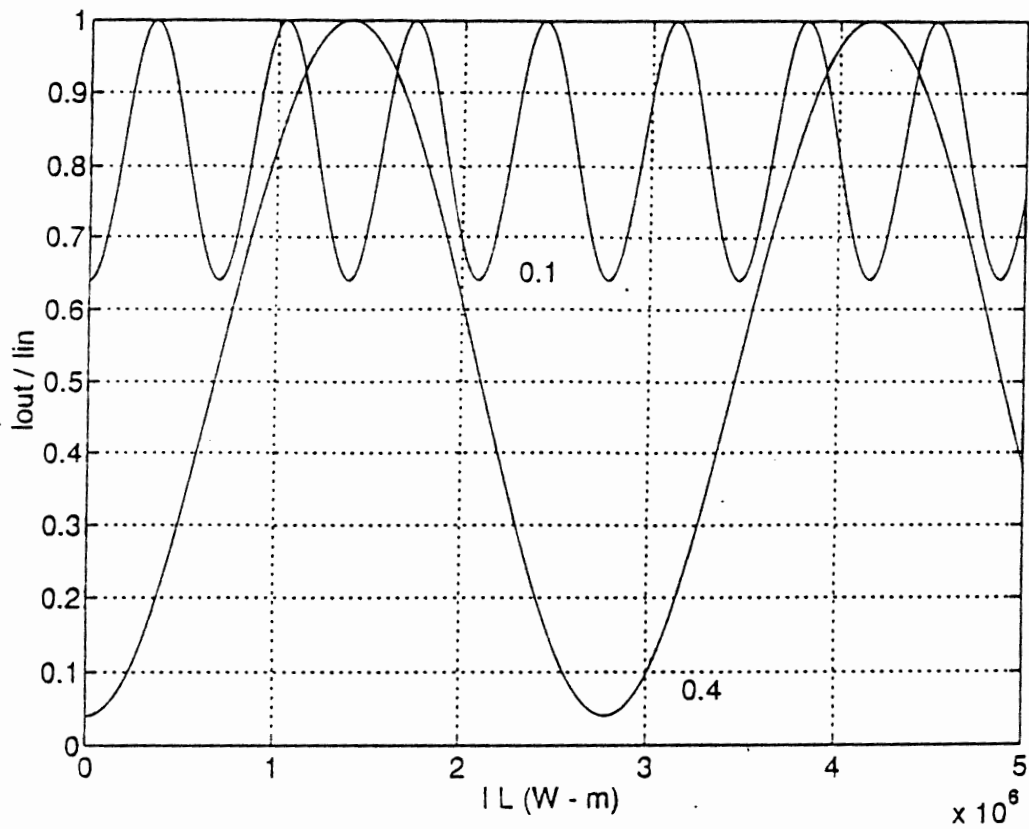


Figure 4. Transfer Function of the Nonlinear Optical Loop Mirror for Couplers with Splitting Ratio of 90 : 10 & 60 : 40

propagating fields has been neglected.

Polarization Consideration.

It has been demonstrated that high intensities are required for switching. It has also been categorically stated earlier that a coupler with a splitting ratio of 50 : 50 is not useful for switching purposes. The aim of this section is to reconsider the same configuration as in Figure 3 with a coupler splitting ratio of 50 : 50 and consider its operation in the linear regime when the polarization of the interfering signal⁶ is changed using retarder plates.

With a coupler splitting ratio of 50 : 50, 50% of the light travels in the clockwise direction and the remaining 50% of the light travels in the counter-clockwise direction. Light coupled across the waveguide suffers a $\pi / 2$ phase lag with respect to the light travelling straight through. The transmitted intensity in port 2 is therefore the sum of the clockwise field of arbitrary phase ϕ and the counter-clockwise field of relative phase $\phi - \pi$. This results in zero transmitted intensity and by conservation of energy all input light is reflected back along port 1.

Consider the propagation of an instantaneous field vector at an angle of θ to the y axis (a) (see Figure 5). Light is split equally by the coupler to form two fields propagating in opposite directions shown by the solid vectors in (b) and (c), where the phase of (c) is delayed by $\pi / 2$ with respect to (b). These fields pass each other midway around the loop (d) and (e), at angles of $-\theta$ and $+\theta$, respectively, and continue around the loop to re-enter the coupler with field vectors again aligned

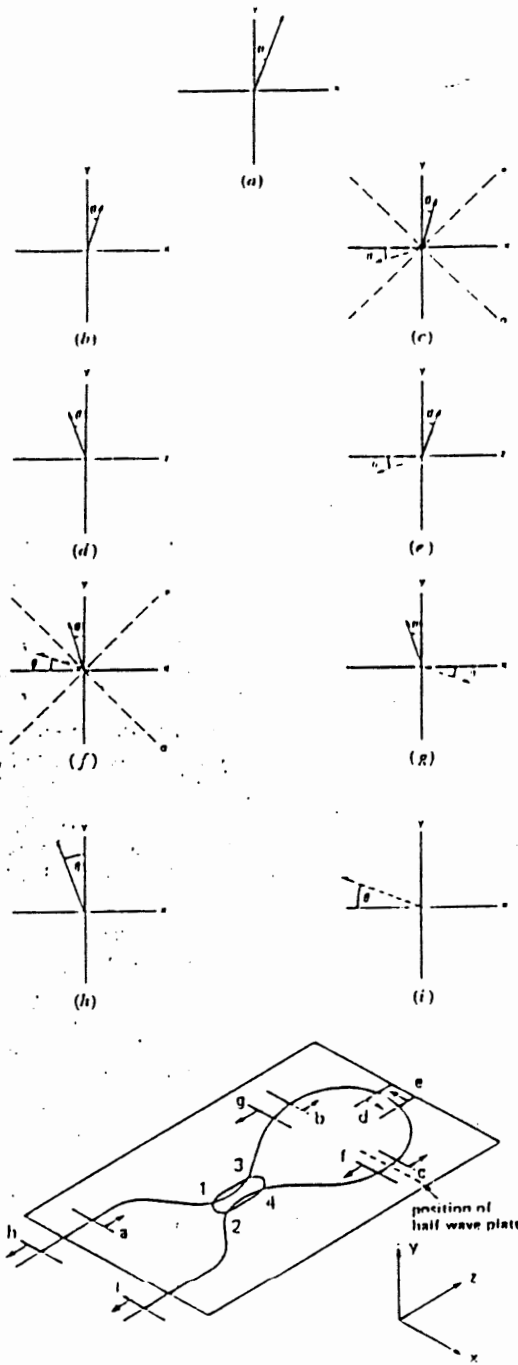


Figure 5. Propagation of Instantaneous Field Vector Around the Loop

but now at an angle of $-\theta$ (f) and (g). With no fiber birefringence, the path length for each counter rotating field is identical and the phase difference ($-\pi / 2$) between the fields is preserved. This results in all light being reflected along port 1 (h), with a rotated polarization of $-\theta$.

Now the effect of birefringence in the loop is considered. It is assumed that birefringence occurs near port 4 of the coupler between the (f) and (c) in Figure 5. Birefringence causes a variation of the optical path length with the polarization angle. Incident light polarized along the fast axis of a discrete half-waveplate will suffer a π phase difference with respect to the light incident along the orthogonal slow axis. If a discrete half-waveplate or polarization controller were placed in the loop with its fast axis at an angle 45° , then light incident at an angle θ will produce two counter propagating fields incident on the waveplate at angles $+\theta$ and $-\theta$. These two field vectors are both rotated in the same direction such that on exit from the waveplate their field vectors point inside the loop at angles $-90 - \theta$ and $-90 + \theta$ as shown by the dashed vectors of (c) and (f). When these fields re-enter the coupler their field vectors are again parallel but they now point in opposite directions which is equivalent to an additional phase difference of π between them. This relative phase difference is as though the light originally entered a non-birefringent loop from leg 2, and therefore light is totally transmitted along leg 2 polarized at an angle of $-90 + \theta$. The reflectivity is thus zero. Thus for any retardation that occurs between 0 and π light will be partially reflected or transmitted. This discussion proves that it is possible to obtain polarization based switching. If polarization preserving fiber is used along

with a half-wave plate the loop can be adjusted to the transmitting mode in the linear regime. It is emphasized that depending on the birefringence in the loop, the transmitting properties of the loop can be adjusted. At low powers with no birefringence, all power is reflected. At high powers with no birefringence, the loop operates in the transmitting mode. At low powers with an effective birefringence that acts like a half-waveplate, the loop transmits all the input power. With the same birefringence, when the input signal power is increased, the loop begins to partially reflect the input power. It has also been speculated that the polarization sensitive properties of the loop might be the cause for the instabilities⁷ observed in the lasers that rely on Nonlinear Optical Loop Mirror as the passive mode-locking element.

The NOLM has also been used in a variety of configurations for switching applications⁸. The NOLM can be used as an ultra-fast switching device when a coupler with a switching ratio of 50 : 50 is used and differential phase shift is induced by superposing a strong signal on one of the counter propagating beams. For efficient switching the phase shift produced due to cross phase modulation should be very high, and this can happen only at high intensities.

From the transmission curves of the device it is observed that as the coupler ratio is changed the switching contrast ratio suffers. To obtain good contrast ratio it is necessary that both the interfering signals be of equal intensity. This is possible only by the usage of a 50 : 50 coupler. But the usage of such a coupler results in no differential phase shift. Hence it is seen that the two requirements that are necessary for efficient operation of the device are conflicting. It should also be noted that very

high intensity is required to switch a pulse. Thus a device that can overcome the above stated limitations and that which can switch powers at low intensities is sought.

Nonlinear Amplifying Loop Mirror

As seen earlier it is necessary to improve the NOLM because of the high switching intensities required. Since fiber is a nonlinear medium one way of introducing asymmetry is to introduce an amplifier asymmetrically in the NOLM. The amplifier used is the Erbium Doped Fiber Amplifier (EDFA). For the present purposes the EDFA introduced will be considered as a simple lumped gain element and the properties of the EDFA itself will be considered in the next chapter. The aim of this section is also to address the advantages offered by the NALM² as compared to the NOLM and to study its operation. This section will also look at the response of the NALM. The effect of third order dispersion is also considered.

The NALM is a significant improvement over the NOLM, in that it switches more efficiently than the NOLM and it amplifies. One way of looking at the NALM is as a saturable reflector. Figure 6 shows the schematic of the NALM. It is seen that an amplifier is added asymmetrically to the NOLM. Without the amplifier, the schematic is similar to a Sagnac interferometer. For this configuration to act as a switching device, a differential phase shift is needed between the two counter propagating beams so that when the two beams interfere in the coupler after traversing the loop, light emerges from leg 2 and not from leg 1. Phase shift occurs

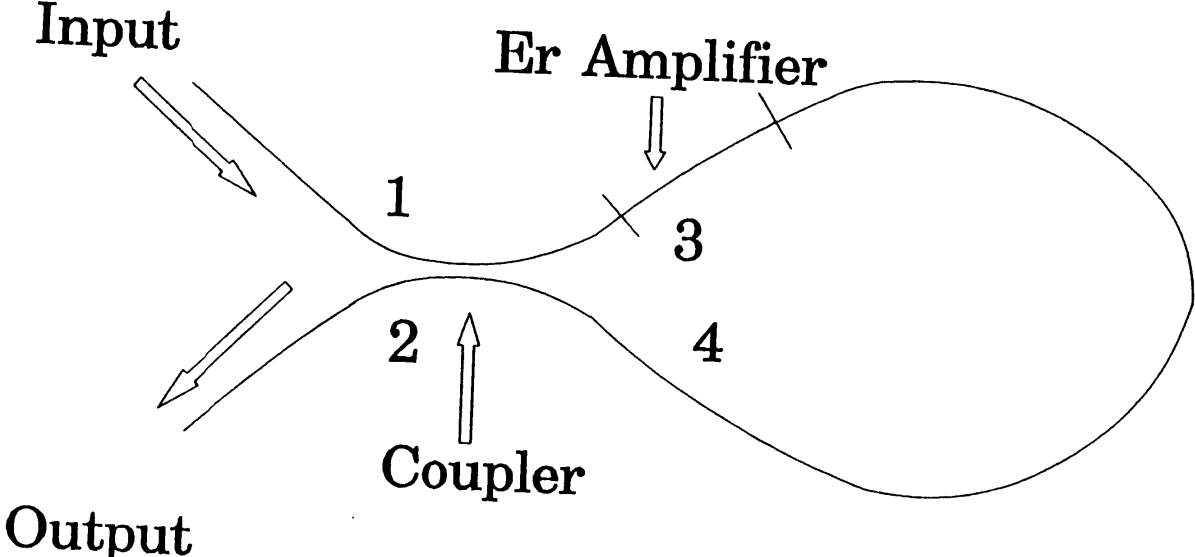


Figure 6. Schematic of the Nonlinear Amplifying Loop Mirror

because of a nonlinear process known as self-phase modulation, wherein the refractive index encountered by the pulse is dependent on its intensity. To illustrate this phenomena consider two pulses of equal intensity travelling in two fibers of exactly the same length. Both the pulses will travel with the same group velocity and hence traverse the same optical path length. At the end of the fiber if these two pulses are made to interfere, they will interfere constructively as there is no differential phase shift between the two pulses. Now if the intensity of one of the pulses is increased, the optical path length encountered by the signals is not the same, since the refractive index encountered by the high intensity pulse is different than that encountered by the low intensity pulse. As the pulses travel a distance L in the fiber this difference in the refractive index encountered by the pulses will manifest itself as a phase difference between the two pulses. If these two pulses are made to interfere, an interference pattern will be observed. This is the key to understanding the operation of the NALM. It is also well known that with changing intensities of the interfering beams, the contrast ratio suffers. So to obtain good contrast ratio in an interference pattern, it is necessary that the two interfering beams be of equal intensity. These points should be borne in mind in the following section. In view of the conflicting requirements needed for efficient operation of the NOLM an improvement is sought.

The improvement is the Nonlinear Amplifying Loop Mirror (NALM). Wherein the interfering pulses are of equal intensity but differential phase shift accumulates because the intensity of the pulses as they traverse the fiber is different. This is achieved by placing an amplifier asymmetrically in the NOLM and by using a

50 : 50 directional coupler. Pulse from leg 1 is split by the coupler into two. The clockwise propagating pulse is amplified before it traverses the length of the loop whereas the counter-clockwise propagating pulse travels around the loop with low intensity. But before re-entering the coupler, the two pulses will be of equal intensity as the low intensity pulse is amplified just before re-entering the coupler. To illustrate this process, consider a pulse of intensity I_0 at port 1, split into two pulses of intensity $I_0 / 2$. The clockwise propagating pulse is amplified and its intensity after emerging out of the amplifier of gain G is $GI_0 / 2$. So the intensity of the clockwise propagating pulse as it travels around the loop is $GI_0 / 2$. Since G is very high, (30 - 40 dB), the intensity is high enough for the accumulation of phase shift due to self-phase modulation. Neglecting the effects of dispersion in the fiber, the intensity of the pulse as it re-enters the coupler at port 4 is $GI_0 / 2$. The counter-clockwise propagating pulse is of intensity $I_0 / 2$ as it travels from port 4 to port 3. Since the intensity of this pulse is low the effects of self-phase modulation can be neglected. This pulse at the end of its journey around the loop enters the amplifier and is amplified. Therefore the intensity of the pulse as it re-enters the coupler is also $GI_0 / 2$. Thus it is seen that both the interfering pulses are of equal intensity and there is a differential phase shift accumulated. Therefore both the disadvantages of the NOLM can be overcome by using a NALM.

If the amplifier and pulse lengths are short compared to the total loop length, and the individual pulses do not saturate the amplifier, the phase delays are given by where I_0 is the signal intensity launched into port 1, L is the fiber length, λ is the

$$\delta\phi_c^{NL} = \frac{\pi}{\lambda} n_2 G I_o L \quad (2-13a)$$

$$\delta\phi_{cc}^{NL} = \frac{\pi}{\lambda} n_2 I_o L \quad (2-13b)$$

signal wavelength, and G is the gain of the amplifier. $n_2 = 4.5 \times 10^{-20} \text{ m}^2/\text{W}$ for silica fibers at $1.06 \mu\text{m}$. It is seen that the clockwise propagating beam experiences a g-times larger phase delay than does the counter-clockwise propagating light. Note that the polarization has not been considered and it is assumed that the input polarization is linear and that the fiber is polarization preserving. Polarization consideration discussed in the earlier section will also apply to the NALM. For complete switching to occur the phase difference between the two beams is required to be π . Input intensity needed for complete switching (I_π) is given by

$$I_\pi = \frac{\lambda}{n_2 L (G-1)} \quad (2-14)$$

In case the fiber is not polarization preserving, mechanical polarization manipulators are used to adjust the polarization. It should be emphasized here that the polarization manipulators can be used to introduce a phase-bias in the loop. This can be done by introducing a half-wave plate in the loop. Thus at low intensities the loop would be transmitting, but as the intensity increases the transmission decreases.

It can be shown that the transmission of the loop is given by

$$I(t) = G I_o(t) \sin^2 \left[\frac{\pi}{\lambda} n_2 (G-1) I(t) L \right] \quad (2-15)$$

It is seen that even though the input intensity is I_o , the intensity of the pulse exiting

the loop at full switching is $G_{I_0}(t)$. Thus the loop also acts like an amplifier. Instead of introducing gain in the loop, asymmetrical loss can also be introduced in the loop by an attenuator, but the whole device would then be attenuating. But under certain conditions this device is preferred over the regular NALM.

The most important characteristic of the loop is its transmission characteristic (Figure 7). The gain of the Erbium amplifier was assumed to be 40 dB. The length of the loop used for the simulation is 400 m. The plot also shows the reflected power and the total power to illustrate the consistency of the plots. It is seen that the input signal powers required to induce switching is on the order of hundreds of microwatts. This is one of the main advantages of the NALM over the NOLM.

A glance at the transmission characteristics reveals that the NALM acts like a saturable reflector because the transmission of the loop increases with increasing input powers. The NALM acts like an intensity dependent mirror. At low intensities the transmission is low, whereas at high intensities the transmission is high. This characteristic of the loop is important for its action as a mode-locking element in the F8L. Also of interest are the characteristics of the pulses transmitted through the NALM. It has been explained earlier that at low intensities the loop transmission is low, but at high intensities its transmission is high. This characteristic is also important for the pulse shaping that occurs in the NALM. The intensity of the pulse varies in the envelope. Assuming the pulse is Gaussian in distribution, the intensity is maximum at the center and decreases towards the sides of the pulse. Since the NALM acts like an intensity dependent mirror, that part of the pulse with high

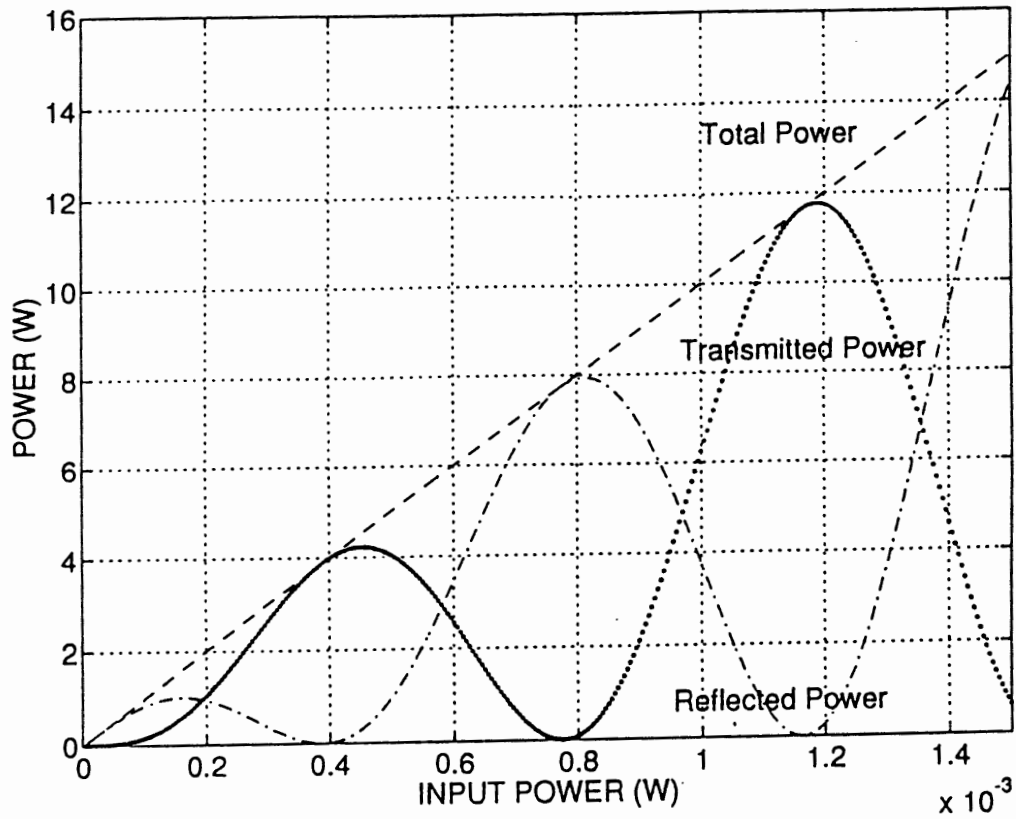


Figure 7. Transmission & Reflection Characteristic of the Nonlinear Amplifying Loop Mirror

intensity is transmitted whereas the low intensity part of the pulse is reflected. The effect is that each time a pulse goes through the NALM, the pulse width decreases. This is very important in understanding why the F8L produces ultrashort pulses. It is therefore instructive to examine the pulse characteristics for the NALM made of different fibers like dispersion shifted, and non-dispersion shifted fibers. For a dispersion shifted fiber, $\beta_2 = -1.5 \text{ ps}^2/\text{km}$ and $15 \text{ ps}^2/\text{km}$ for a non-dispersion shifted fiber. β_2 is the group velocity dispersion parameter related to the dispersion parameter, D , found in literature as⁹

$$\beta_2 = -\frac{\lambda^2}{2\pi c} D \quad (2-16)$$

This is the parameter that dictates the pulse width as the pulse travels along a fiber. The third order dispersion parameter, β_3 is of importance for modeling ultra-short pulses in a fiber. β_3 used for the calculation is equal to $0.01 \text{ ps}^3/\text{km}$ for dispersion flattened fiber. Figure 8 shows the transmitted and reflected pulse for a loop made non-dispersion shifted fiber ($\beta_2 = -15 \text{ ps}^2 / \text{km}$) of length 400 m and an amplifier gain of 40 dB. The width of the input pulse was set at 1.5 ps. At input powers in the range of $550 \mu\text{W}$ complete switching occurs. It is seen that the central part of the pulse is transmitted as explained before. If the input signal intensity is less than that required for complete switching, the central part of the input pulse is not completely transmitted. Simulations to study switching in the absence of β_3 , the third order dispersion, were made but this had no considerable effect because the width of the input pulse is of the order of picoseconds. The polarization of the input signal was

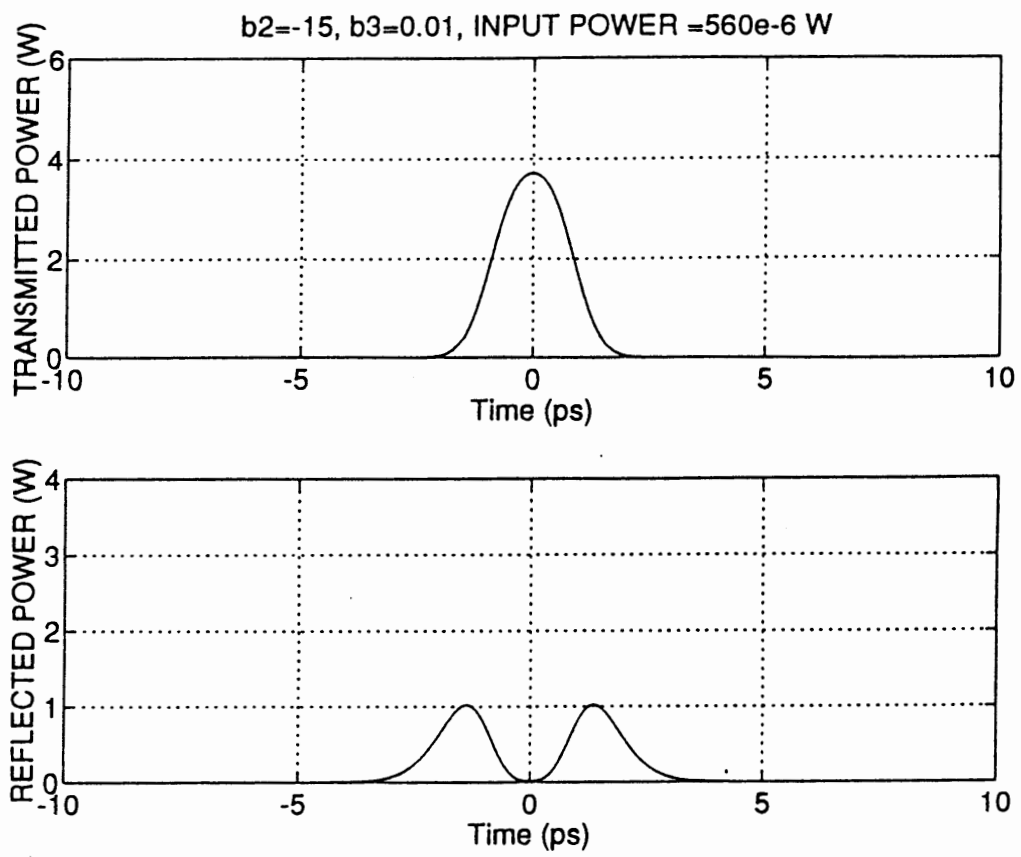


Figure 8. Transmitted and Reflected Output of NALM

assumed to be linear and it is was also assumed that it is preserved as the signal travels along the fiber. The loop is assumed to be in the reflecting mode at low powers. The reflected pulse is shown to illustrate the conservation of energy.

FOOTNOTES

¹N. J. Doran and David Wood, Opt. Lett. 13, 56 (1988).

²Eugene Hecht and Alfred Zajac, Optics (Addison-Wesley, Reading, MA, 1979), Chapter 9.

³Eugene Hecht and Alfred Zajac, Optics (Addison-Wesley, Reading, MA, 1979), Chapter 4.

⁴M. E. Fermann, F. Habrel, M. Hofer and H. Hochreiter , Opt. Lett. 15, 752 (1990).

⁵Irl N. Duling III, Opt. Lett. 16, 539 (1991).

⁶David B. Mortimore, Journal of Lightwave Technology, 6, 1217, (1988).

⁷N. Finlayson, B. K. Nayar and N. J. Doran, Opt. Lett. 17, 112 (1992).

⁸M. N. Islam, E. R. Sunderman, R. H. Stolen, W. E. Pleibeland J. R. Simpson, Opt. Lett. 14, 811 (1989)

⁹G. P. Agrawal, Nonlinear Fiber Optics (Academic Press, Boston, 1989), Chapter 3

CHAPTER III

ERBIUM DOPED FIBER AMPLIFIERS

It has been observed in the earlier section that the NOLM requires very high intensity light to exhibit nonlinear effects. In order to increase the efficacy of the NOLM, Fermann et. al¹, in 1990, proposed an improvement called the Nonlinear Amplifying Loop Mirror, which incorporated an Erbium Doped Fiber Amplifier. The aim of this section is to examine the properties the EDFA itself which is fast becoming a mainstay in communication lines. In a communication system, the attenuation imposed by the guiding medium on the information carrying signal necessitates the incorporation of a repeater station. Repeater stations are used to filter the noise components from the signal, amplify, and retransmit the signal to its destination. Present repeater technology for optical communication converts the incoming optical signal into an electrical signal which is filtered, amplified and reconverted into an optical signal for transmission. Since a more efficient way of boosting the signal power is to incorporate in-line fiber amplifiers, there has been a lot of interest in its development. With the realization of attenuation less than 0.25 dB/km at 1.55 μm coupled with the lack of good amplifiers at 1.3 μm has lead to the

development of rare earth doped silica amplifiers at $1.55 \mu\text{m}$. In the late eighties the efforts of researchers culminated with the development of an Erbium Doped Fiber Amplifier at the University of Southampton². The subject of rare earth doped fiber amplifiers has recently received growing attention in the technical literature and at international scientific conferences. The key component of most of the passively mode-locked soliton generators and ultra-fast optical switches is the EDFA. The much talked about soliton transmission will be made possible by these fiber amplifiers.

There are two other types of optical amplifiers, namely, semiconductor and Raman fiber amplifiers. A semiconductor laser amplifier has the advantage of smaller size and lower power consumption. However, it is sensitive to polarization and have a large insertion loss when connected to transmission fibers. Therefore, they are most suitable for use when combined with optical integrated circuits and optoelectronic integrated circuits. The main disadvantage of Raman amplifiers is the high powers required to obtain useful gain. The reason for this is the small magnitude of the Raman gain coefficient.

Erbium belongs to the class of elements known as Rare Earths. Rare earths or Lanthanides are a set of 15 elements occupying the penultimate row of the periodic table. They range from Lanthanum (La) with an atomic number of 57 to Lutetium (Lu) with an atomic number of 71. All the rare earth atoms have the same outer electronic structure of $5s^25p^66s^2$, which are filled shells. The number of electrons occupying the inner 4f shell dictate their optical characteristics. La has zero and Lu

has fourteen 4f electrons. Optical absorption and emission cause transitions in the 4f shell. Glasses, which form the host materials for the rare earth doped fibers, consist largely of covalently bonded molecules, which form a disordered matrix, having a wide range of bond angles. Order is only displayed over short ranges at the local level. The rare earth ions usually exist as network modifiers, or are interstitially situated in the glass network³.

At extremely low doping levels of the active species, the ground state can become depleted in circumstances where the total number of available ions is less than the number of incident photons. Signal amplification is limited by the availability of ions. Therefore it seems that increasing the dopant levels would improve the gain. There are two problems involved with high dopant levels. The first problem is concentration quenching. At high dopant levels there is non-radiative cross relaxation between the adjacent closely spaced rare earth ions, causing a reduction in the population of the upper lasing levels. The second problem is the crystallization that occurs within the glass matrix. The concentration of the rare earth ions that can be incorporated in the glass matrix without crystallization depends on the glass system.

Erbium is a three level system. The pump laser promotes electrons from the ground state to one or more pump bands which are above the upper lasing level. Electrons then decay, usually non-radiatively, to the upper lasing level. The spontaneous lifetime of the upper lasing level must exceed that of the pump bands by a significant margin to allow heavy population inversion of the upper level. When a photon is present at the laser wavelength, a stimulated photon is obtained. In a three

level system, the lower lasing level is either the ground state or a level so close to the ground state that it has a low thermal population. Four level lasing systems also exist, an example of which is Neodymium. A consequence of the number of levels involved is the fiber length dependence on the gain. In a three level system there is an optimal length which facilitates maximum gain. In an end pumped three level fiber laser, the number of available pump photons, and hence population inversion will be greatest at the launch end. If the fiber is too short, there will be insufficient absorption of the launched pump radiation and this results in inefficient utilization of pump power. If, on the other hand, the fiber is too long, at the output end the pump power levels are below the threshold pump powers, hence the fiber ceases to be transparent to input signal. There will be net absorption of the lasing photons to repopulate the upper lasing level, and so the available output power is decreased. Threshold power (P_{th}) is defined as the amount of pump power required to make an infinitesimally small length of doped fiber transparent to the signal. A specified length of doped fiber is said to be optimally pumped when the pump power at the end of the fiber is equal to the threshold power. At the launch end, the pump power is greater than the threshold power and amplification occurs. Along the length of the fiber, the pump power decreases, and a point is reached when the pump power in the fiber is equal to the threshold power. The signal grows in amplitude as it travels along the fiber, although the signal power increases, dG / dL decreases, (G is the gain of the amplifier and L , the length of the amplifier), and finally crosses zero at the end of the optimally pumped fiber. If the fiber is too long, it is no longer

transparent to the signal and part of the amplified signal is absorbed. Thus it is critical that the length of the fiber and the pump power be carefully chosen.

Another absorption process that does not originate in the ground state of the lasing ions, but from a higher lying excited state, most usually the upper laser level in the ion of interest is the Excited State Absorption (ESA)³. ESA can affect oscillators and amplifiers in two distinct ways: through parasitic absorption at the pump wavelength (pump ESA) or at the wavelength of the amplified signal or the laser output signal (signal ESA). The effect of these two processes is different, although both will result in a reduction in device efficiency. Excited state absorption occurs when the electrons pumped to the higher levels absorb pump or signal radiation to reach a higher level. Figure 9 illustrates pump ESA. The electrons that are excited from the higher states either by the absorption of pump or signal wavelength do not contribute to the gain process and lead to a decrease in the efficiency. ESA is of particular significance to systems like Erbium. Potential ESA transitions arise from the metastable ${}^4I_{13/2}$ level. Several of these transitions coincide with pump transitions from the ground state. The effect of pump ESA can be severe for an amplifier pumped at these wavelengths. ESA will have particularly detrimental effect on the efficiency of the high gain amplifiers, which will be pumped close to full inversion. For Erbium in silica, the only levels that are appreciably populated are the ground state and ${}^4I_{13/2}$ levels, so the build up of population in other intermediate levels can be neglected. Although most of the absorption bands of Erbium overlap with the ESA bands, the 980 nm band has very little pump ESA. Hence the 980 nm absorption line

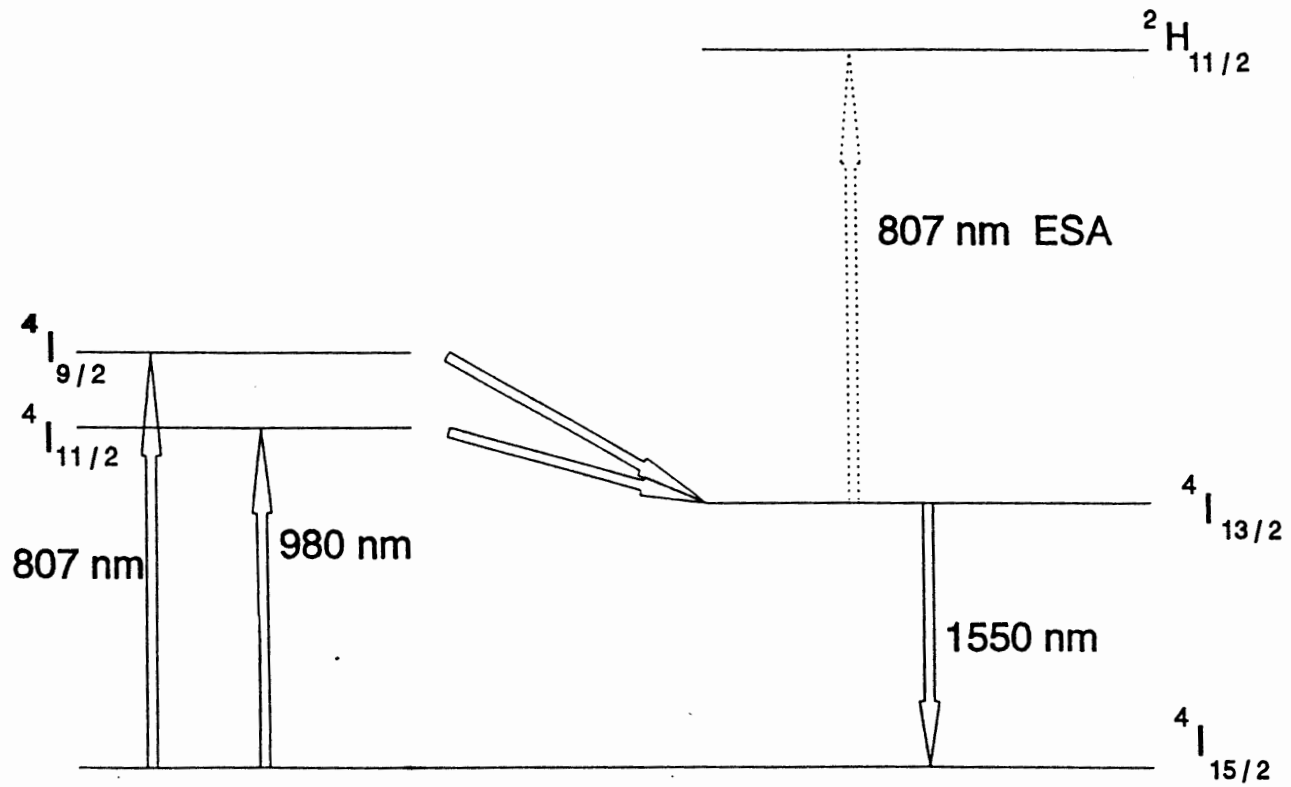


Figure 9. Illustration of Pump ESA

is used for pumping the EDFA⁶. Signal ESA is not dealt with because it is insignificant for EDFA in the wavelength range of 1.5 - 1.6 μm . But it becomes significant for wavelengths longer than 1.6 μm .

As both the ends are accessible in a fiber, there are three basic EDFA pump configurations⁴. They are classified by their pump and signal propagation direction. The signal light co-propagates with the pump light in the forward pumping configuration, and counter propagates with the pump light in backward pumping configuration. The third configuration is bi-directional pumping. Forward pumping is profitable for good noise performance and backward pumping for gain considerations. The characteristics that are of interest are: gain dependence on pump power and gain dependence on length. The importance of gain dependence on length has been explained earlier. A quantitative examination of the following characteristics will shed more light on the EDFA performance and will lead to an algorithm for the design of practical EDFA systems that can be used in a communication system.

Assuming that the emission cross section at the pump wavelength is zero, the normalized pump light intensity I_p and the normalized signal light intensity I_s of the forward pumping configuration is given by⁴

$$\frac{dI_p}{dz} = \frac{I_s - 1}{1 + 2I_s + I_p} \alpha_p I_p \quad (3-1a)$$

$$\frac{dI_s}{dz} = \frac{I_p - 1}{1 + 2I_s + I_p} \alpha_s I_s \quad (3-1b)$$

where α_s , α_p and z are the signal absorption coefficient, pump absorption coefficient

and longitudinal fiber coordinate, respectively. From the above two equations the following relations are obtained.

$$\alpha_p L = \frac{P_i}{P_{th}} - \frac{P_{out}}{P_{th}} + \ln \left(\frac{P_i}{P_{out}} \right) \quad (3-2a)$$

$$\frac{P_i}{P_{th}} - \frac{P_{out}}{P_{th}} - \log \left(\frac{P_i}{P_{th}} \right) = - \frac{\alpha_p}{\alpha_s} \frac{\ln 10}{10} G \quad (3-2b)$$

Eqn (3-2a) describes the pump decay with respect to the longitudinal coordinate. Eqn (3-2b) relates the pump change to the signal change. Experimentally the value for P_{th} is obtained by measuring α_p and the pump power P_o , which makes the erbium fiber transparent. Using the above two equations and setting $G = 0$, we obtain

$$P_{th} = P_o \frac{(1 - e^{-\alpha_p \frac{L}{2}})}{\alpha_p \frac{L}{2}} \quad (3-3)$$

The relation between P_o / P_{th} and the normalized length is shown in Figure 10.

These equations are very useful in the design of EDFAs because they relate, normalized pump input power, normalized gain and normalized length of the fiber.

Figure 11 shows the dependence of normalized gain on normalized pump power. The axes are marked as Normalized Pump Power (P_i / P_{th}) and Normalized Signal Gain ($\alpha_p G / \alpha_s$). The family of graphs is obtained by varying the normalized length ($\alpha_p L$) of the fiber. This has been done in order to make the graphs presented independent of the characteristics of the individual fiber. As expected with any

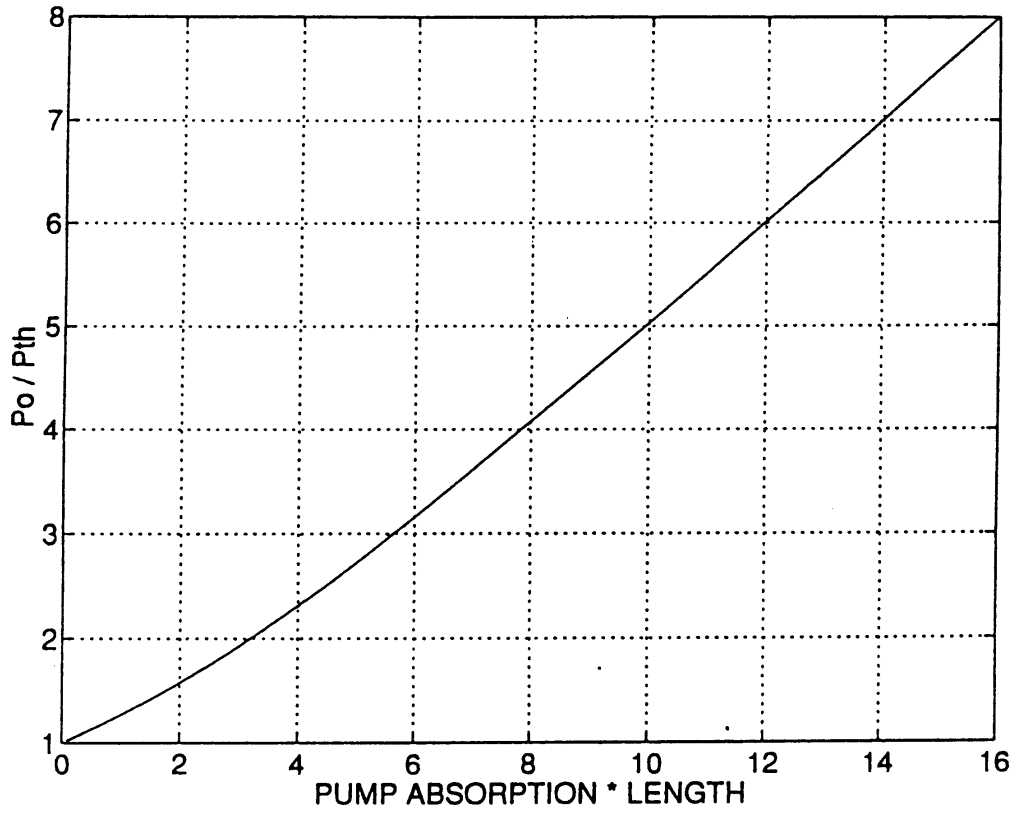


Figure 10. Normalized Length vs Normalized Output Power

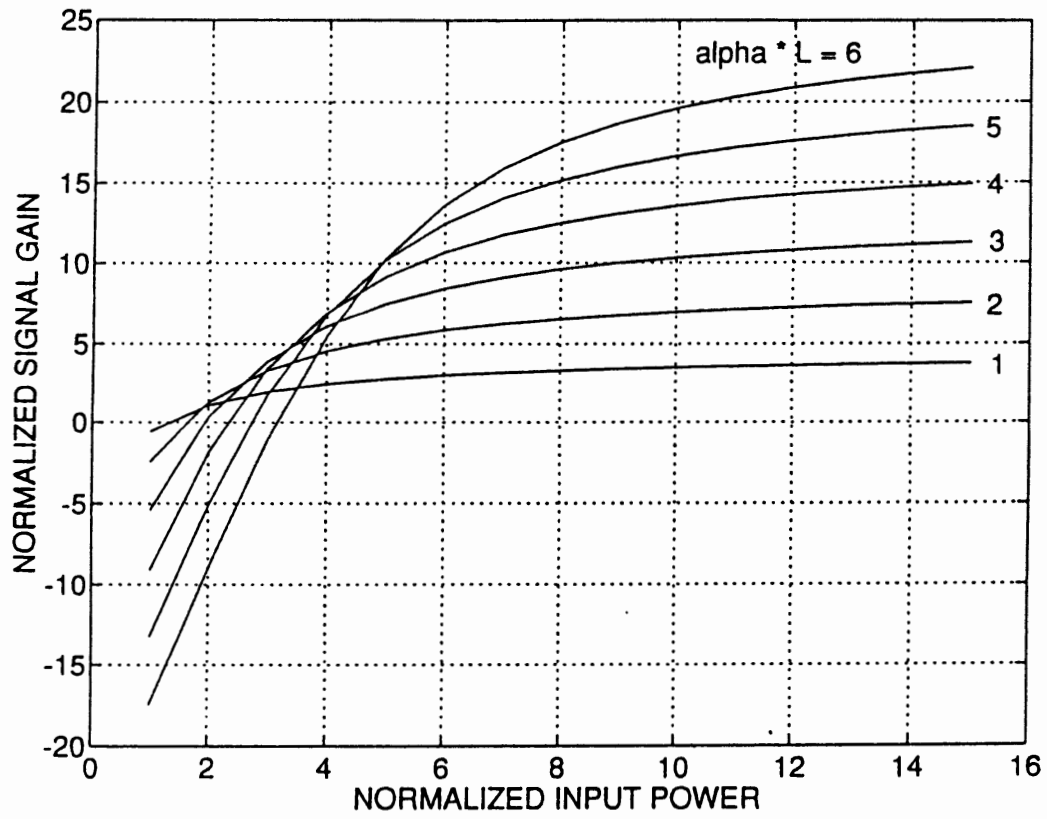


Figure 11. Normalized Gain vs Normalized Pump Power

amplifier the gain saturates with increasing pump powers. Figure 12 shows the dependence of normalized gain on normalized length of the EDFA for fixed and normalized pump powers. This graph reveals the importance of selecting the optimum length of the EDFA. It is seen that using Eqns (3-2a) and (3-2b), design of EDFA is simple. Figure 13 shows a plot of engineering interest. The advantage of this graph is that knowing the length of fiber available, the necessary pump power required to obtain optimum gain can be obtained along with the optimum gain itself.

The cases that have been considered till now are the cases where the effect of signal on pump decay has been neglected and hence known as the unsaturated case. For the saturated case, where the effect of signal on the pump is taken into account, the following equations can be obtained⁴.

$$\ln\left(\frac{P_{sout}}{P_{sth}}\right) - \ln\left(\frac{P_{sin}}{P_{sth}}\right) + \left(\frac{P_{sout}}{P_{sth}} - \frac{P_{sin}}{P_{sth}}\right) = \frac{\alpha_p}{\alpha_s} \left(\frac{P_i}{P_{th}} - \frac{P_{out}}{P_{th}} + \ln\left(\frac{P_{out}}{P_i}\right)\right) \quad (3-5)$$

This equation relates the signal input power (P_{sin}), signal output power (P_{sout}), pump input power (P_i) and pump output power (P_{out}). P_{th} is the threshold pump power defined earlier and P_{sth} is the signal power beyond which the decay of signal tends to be linear instead of being exponential. Using this relation the dependence of normalized pump power on normalized signal output and normalized pump power at constant signal power is obtained. This is shown in Figure 14. For the purposes of calculation α_p / α_s was taken as 2.42⁴.

The relation between normalized signal input power and normalized signal output power at constant input pump powers is shown in Figure 15. It should be

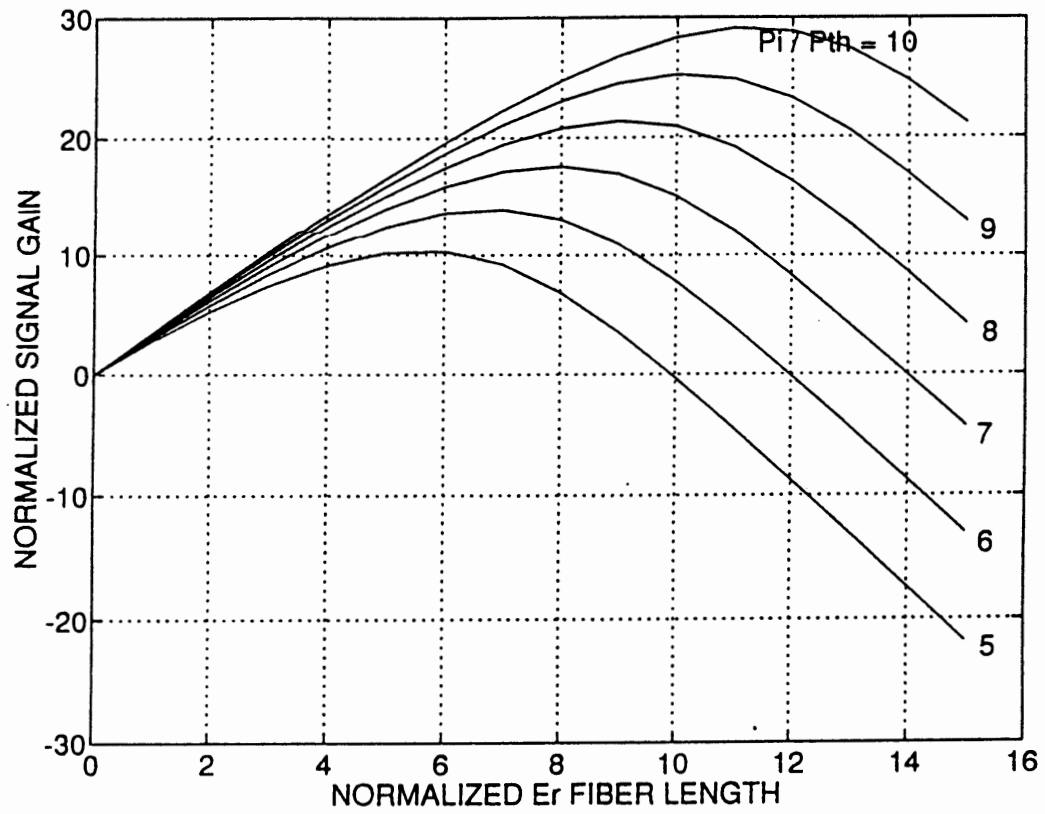


Figure 12. Normalized Gain vs Normalized Length

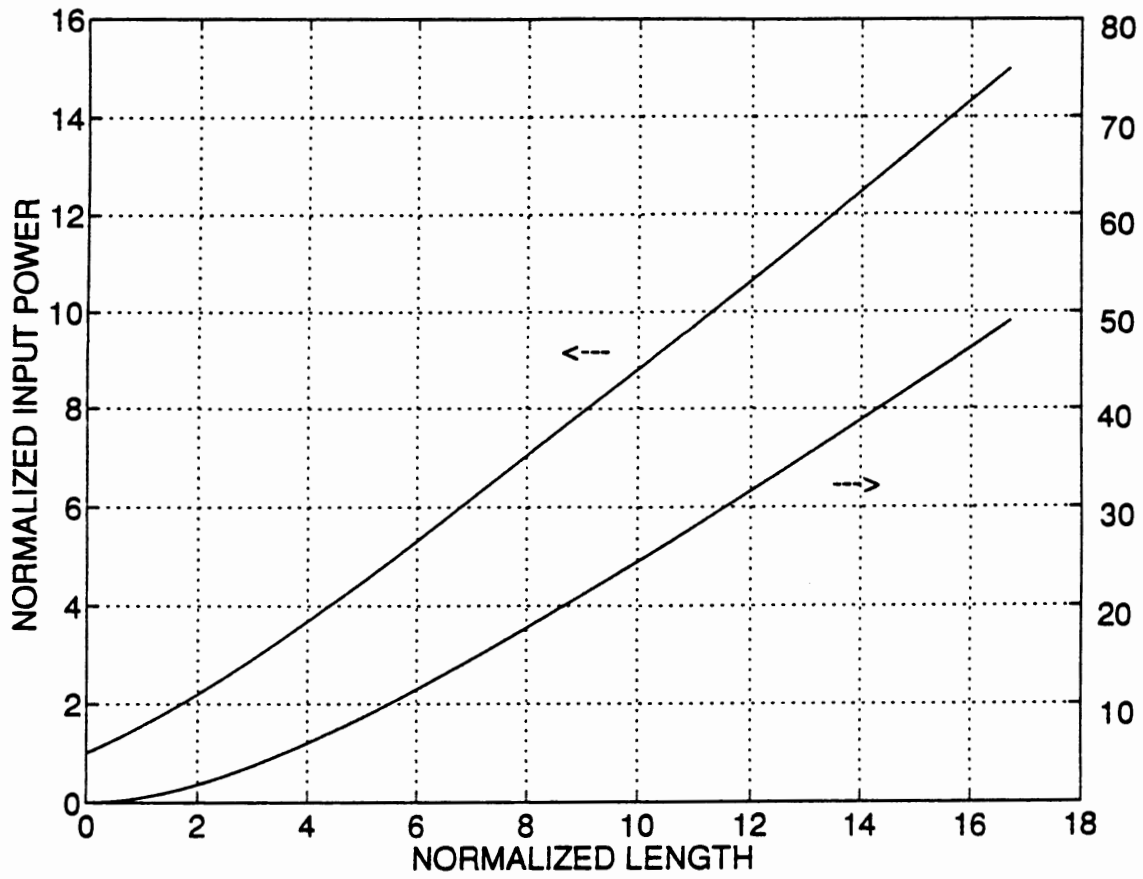


Figure 13. Plot Showing Optimum Gain and Optimum Pump for Normalized Fiber Lengths

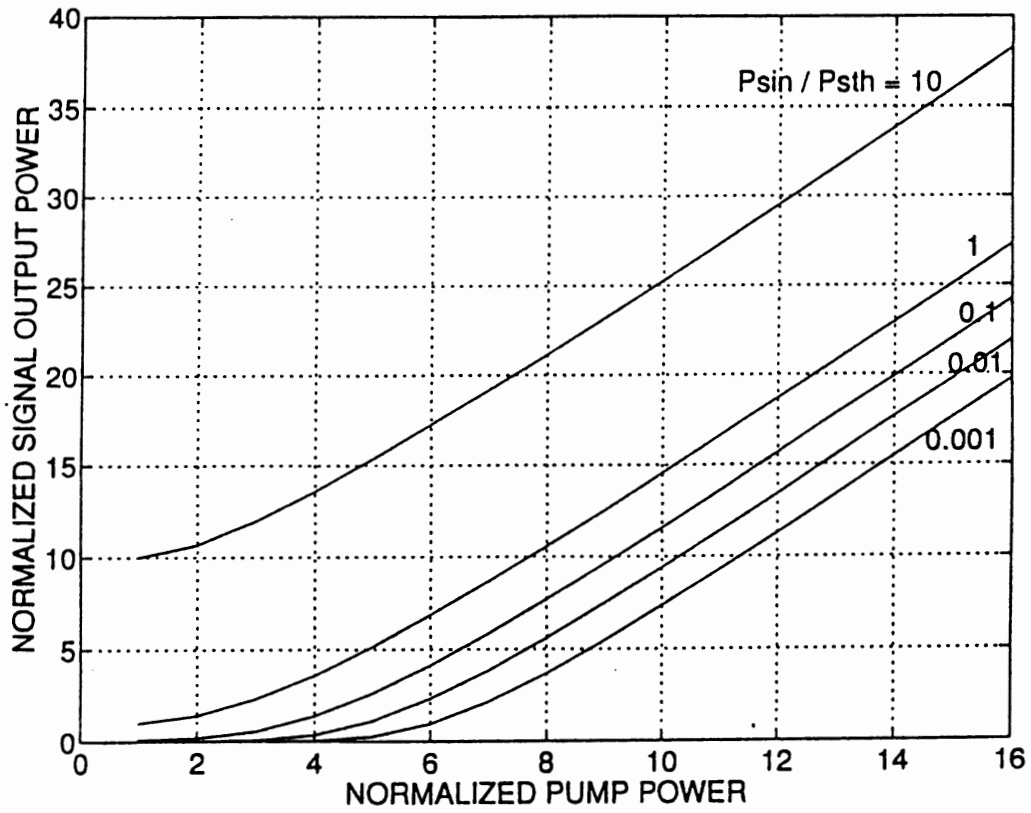


Figure 14. Normalized Signal Output Power vs Normalized Pump Power

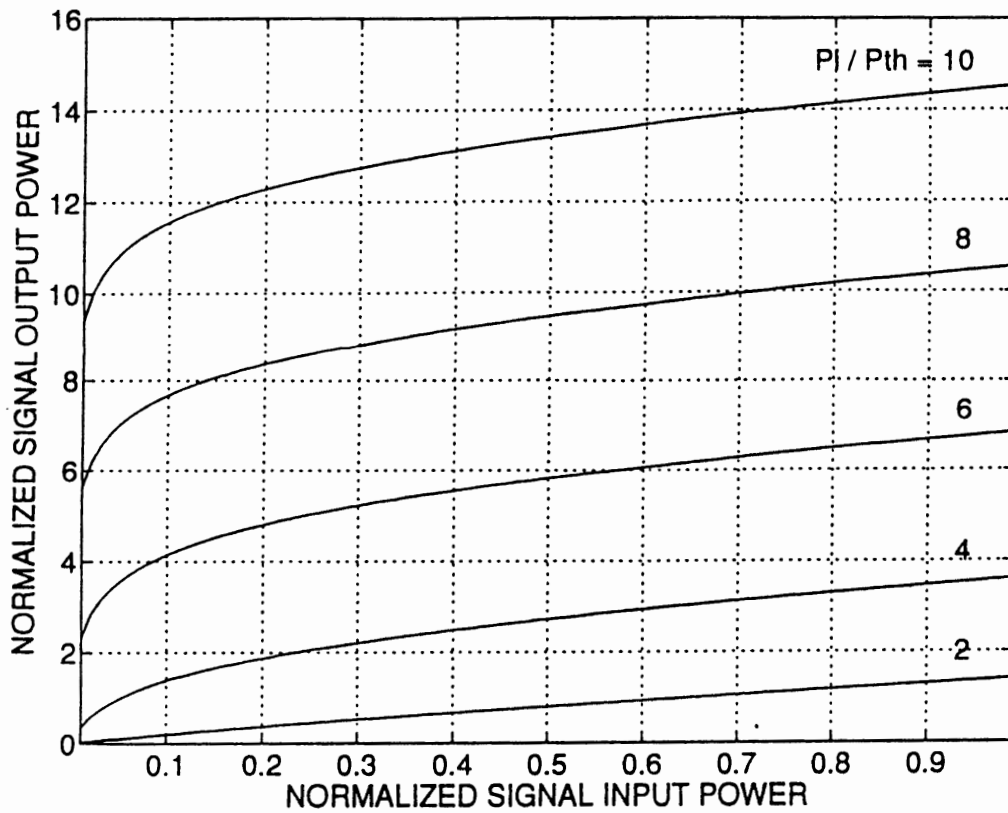


Figure 15. Normalized Signal Input/Output Power Characteristics

noticed here that Figure 15 along the plots with fixed input signal power, the length of the fiber is changing. The output at the fiber end is fixed to P_{th} , i.e. to obtain maximum gain. Therefore along any of the plots the length of the fiber is changing so as to keep the output at the end of the fiber equal to P_{th} . Since this does not convey useful information an improvement is sought.

Figure 16 shows the dependence of gain on the fiber coordinate, which is the analogous to Figure 12. of the unsaturated system. The configuration under consideration till now has been the one wherein the signal and the pump are co-propagating. For the case of counter propagating signal and pump similar relations can be obtained. It has been observed⁷ that the gain that can be obtained for the same amount of pump power is higher for the counter-propagating pump and signal. It is advantageous to use the EDFA in the backward pumping configuration where the signal and the pump are counter propagating. A similar analysis can also be carried out for the case when the pump is bi-directional. In this case the gain that can be obtained is the highest of the two cases that have been considered.

Gain in erbium doped fibers has been shown to be insensitive to the state of polarization of the signal² removing the need for polarization control at the input of the amplifier. The random orientation of erbium ions in the fiber core leads to the averaging out of polarization effects along the length of the fiber. Interestingly, polarization dependent loss mechanism has been reported in erbium fibers⁵. This is commonly referred to as polarization hole burning (PHB). PHB is defined as the difference in gain experienced by the orthogonal polarization components of the

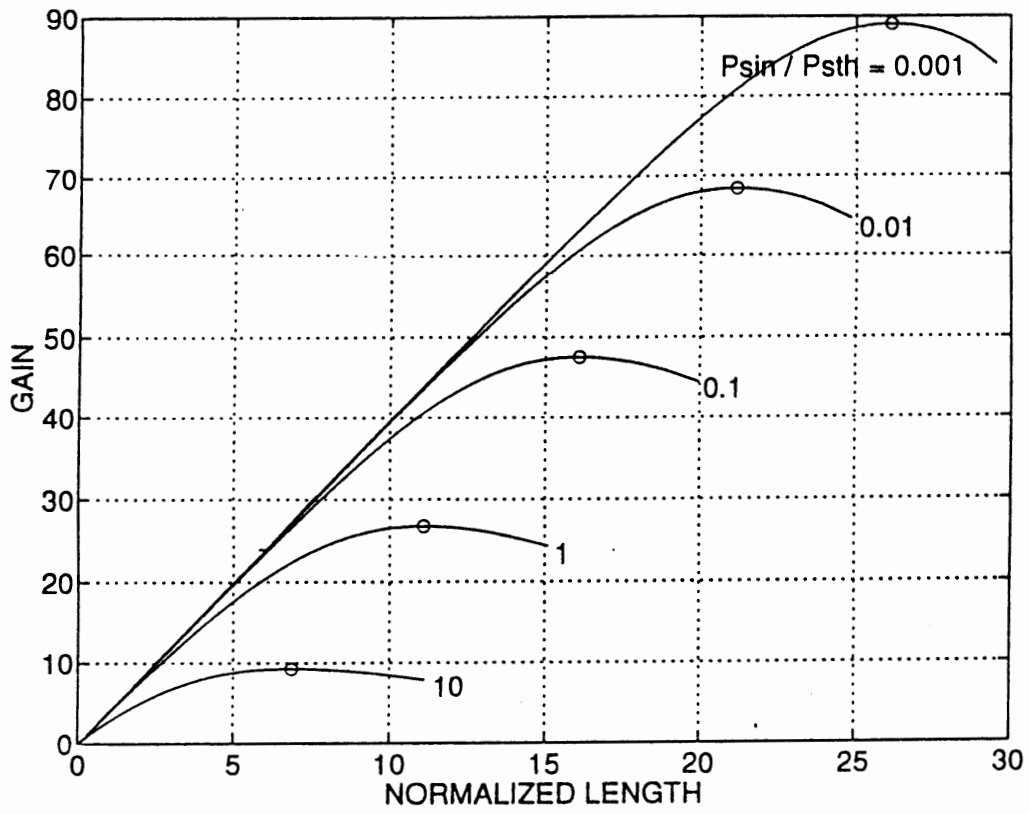


Figure 16. Normalized Gain vs Normalized Length for Saturated Regime

signal. The signal component parallel to the pump experiences lower gain compared to its orthogonal component. The difference is of the order of 0.1 dB. PHB arises from the randomly distributed orientations of erbium ions in the glass matrix and the selective saturation of these ions by a polarized signal. PHB tracks the polarization of the signal through the system. These effects are significant only when the state of polarization is non-circular for both pump and signal. Although the effect of PHB is very small, it is important only for long haul transmission systems. Other interesting effects like spatial- hole burning have also been observed in EDFAs. This leads to mode-hopping in single frequency lasers using EDFAs.

With a thorough understanding of the mechanism of the amplification and the various other processes that occur in erbium doped fibers, an understanding of the basic principles of mode-locking will put all the knowledge accumulated in proper place leading to the F8L.

Mode-locking

The purpose of this section is to explain the concept of mode-locking and examine the importance of a passively mode-locking a laser. This section also investigates the shortest pulse that can be obtained using an EDFA. First mode-locking is discussed and then the advantage of mode-locking with the NALM are investigated.

Any digital optical communication system uses a pulsed source onto which

information is encoded. The most direct method of obtaining pulsed light from a laser is to use a continuous-wave (*cw*) laser in conjunction with an external switch or modulator that transmits the light only during selected short time intervals. Another way is to use a mode-locked laser. Three methods that are commonly used to produce pulsed light are Gain Switching, Q-Switching and Mode-locking. Each of these approaches are discussed in turn and their advantages and disadvantages are enumerated in defense of a mode-locking.

Gain Switching

This is a rather direct approach, the gain is controlled by turning the pump laser ON and OFF. During the ON-times the gain coefficient exceeds the loss coefficient and the laser light is produced. Most pulsed semiconductor lasers are gain switched because it is easy to modulate the electric current used for pumping. Turning the pump on and off is equivalent to modulating the small-signal population difference. At $t < 0$, when the pump is off, the population difference lies below the threshold and oscillation cannot occur. When the pump is turned on at $t = 0$, the population difference increases beyond the threshold value. Once the difference crosses the threshold value, laser oscillation begins and the number of photons per unit volume in the resonator, $n(t)$, increases. The population inversion then begins to deplete so that the rate of increase of population difference slows down. As $n(t)$ become larger, the depletion becomes more effective so that the rate of population difference approaches the steady state value equal to the threshold level. When the

pump is turned off, the population difference decreases below the threshold value and oscillation ceases. It is fairly obvious that an external switch is needed to control either the pump current or laser. This warrants the need for another external circuitry. It is also seen that the maximum repetition rate obtainable is dependent on the response time of the switch. It should also be noted that the width of the pulse is proportional to the cavity lifetime.

Q-Switching

A Q-switched laser pulse is obtained by switching the resonator loss coefficient (α_r) from a large value during the OFF-time to a small value during the ON-time. This can be accomplished in a number of ways, such as by placing a modulator that periodically introduces large losses in the resonator. Since the population difference required at threshold is proportional to α_r , the result of switching α_r is to decrease the threshold population inversion from a high value when the resonator is misaligned to a low value when the resonator is perfectly aligned. Thus this method of obtaining pulses also warrants the need for external circuitry.

Mode-locking

Mode-locking is the most efficient way of producing short pulses. As with the other cases it does not require external circuitry to obtain pulses. The main advantage of mode-locking is that it is possible to obtain ultrashort pulses. The shortest pulse that can be obtained is inversely proportional to the gain bandwidth of the amplifier. Thus mode-locking is preferred over other methods of producing pulses in lasers.

Many laser modes can oscillate in a laser, at frequencies that are equally separated by the intermodal spacing $\nu_F = c / 2d$. Although these modes normally oscillate independently, external means can be used to couple them and lock their phases together. The modes are the components of a Fourier-series expansion of a periodic function of time period $T_F = 1 / \nu_F$, in which case they constitute a periodic pulse train.

As said earlier, mode-locking essentially requires that the various longitudinal modes be coupled to each other. In practice this can be achieved either by modulating the loss (amplitude modulation) or optical path length (phase modulation) of the cavity or gain externally. These can be done either actively or passively. In order to understand how a periodic loss modulation inside the cavity can lead to mode-locking, consider a laser resonator having a loss modulator inside the cavity with the modulation frequency equal to the intermode spacing $\delta\nu$. Consider one of the modes at a frequency ν_q . Since the loss of the cavity is being modulated at a frequency $\delta\nu$, the amplitude of the mode will also be modulated at the same frequency $\delta\nu$ and thus the resultant field in the mode may be written as

$$(A + B\cos 2\pi \delta\nu t)\cos 2\pi \nu_q t = A\cos 2\pi \nu_q t + \frac{1}{2}B\cos[2\pi(\nu_q + \delta\nu)t] + \frac{1}{2}B\cos[2\pi(\nu_q - \delta\nu)t] \quad (3-6)$$

Thus the amplitude modulated mode at a frequency ν_q generates two waves at frequencies $\nu_q + \delta\nu$ and $\nu_q - \delta\nu$. Since $\delta\nu$ is the intermodal spacing, these new frequencies correspond to the two modes lying on the either side of ν_q . The

oscillating field at these frequencies, $\nu_q \pm \delta\nu = \nu_{q\pm 1}$, forces the modes corresponding to these frequencies to oscillate such that a perfect phase relationship now exists between the three modes. Since the amplitudes of these new modes are also modulated at frequency, $\delta\nu$, they generate new side bands at $\nu_q + 2\delta\nu = \nu_{q+2}$ and $\nu_q - 2\delta\nu = \nu_{q-2}$. Thus all modes are forced to oscillate with a definite phase relationship and this leads to mode-locking. But this process of extension in frequency domain cannot continue indefinitely. The frequency range of the mode is limited by the gain-bandwidth of the gain medium

Mode-locking can also be understood in the time domain by noticing that the intermodal frequency spacing, $\delta\nu = c / 2d$, corresponds to a time period of $2d / c$ which is exactly one round trip time. Hence considering the fluctuating intensity present inside the cavity, we observe that since the loss modulation has a period equal to a round trip time, the portion of the fluctuating intensity incident on the loss modulator at a given value of loss would after every round trip be incident at the same loss value. Thus, light incident at the highest loss instant will suffer the highest loss at every round trip. Similarly, light incident at the instant of lowest loss will suffer the lowest loss at every round trip. This will result in the build up of narrow pulses of light which pass through the loss modulator at the instant of lowest loss. The pulse width will be approximately equal to the inverse of the gain bandwidth since the wider pulse would experience higher loss in the modulator and the narrower pulses, which would have a broader spectrum than the gain bandwidth, would have lower gain. Thus the above process leads to mode-locking.

Mode-locking has been achieved in a variety of laser cavities using acousto-optic modulators (AOM). The usage of a modulator to mode-lock the laser is known as active mode-locking. Mode-locking can also be obtained using a saturable absorber inside the laser cavity. This technique does not require an external signal to modulate loss in the cavity and is referred to as passive mode-locking. Consider a laser cavity with a cell containing a saturable absorber placed in a cell adjacent to one of the resonator mirrors. Initially the saturable absorber does not transmit fully and the intensity inside the resonator has a noise-like structure. The intensity peaks arising from this fluctuation bleach the saturable absorber more than the average intensity values. Thus the intensity peaks suffer less loss than the other intensity values and are amplified more rapidly as compared to the average intensity. If the saturable absorber has a rapid relaxation time so that it can follow the fast intensity oscillations in the cavity, one can obtain mode-locking. Since the transit time of the pulse through the resonator, T_F is $2d / c$, the mode-locked frequency will be $c / 2d$.

Mathematically, it can be shown that in a mode-locked laser

$$I(t,z) = M^2 |A|^2 \frac{\text{sinc}^2[M(t-z/c)/T_F]}{\text{sinc}^2[(t-z/c)/T_F]} \quad (3-7)$$

where M is the number of longitudinal modes, A , the complex envelope and $T_F = 2d / c$.

This expression is obtained by approximating the laser modes by uniform plane waves propagating in the z direction with a velocity $c = c_o / n$. Taking the sum of all the modes and assuming them to be in phase, the above expression is obtained.

The above expression is a periodic function in time. The pulse width is inversely proportional to the atomic linewidth. If the bandwidth over which the amplification occurs is substantial, then the pulse width that can be obtained will be correspondingly low¹⁰. This is because as the frequency components that constitute the pulse increase the width in the time domain will decrease and this can occur only when the gain bandwidth of the amplifier is large.

Examples of mode-locked lasers are Colliding Pulse Mode-locked (CPM) lasers and fiber lasers involving nonlinear polarization evolution¹¹. In the present context the NALM along with the isolator acts like a saturable absorber. At low intensities light is reflected and is absorbed by the isolator. At high intensities light is transmitted by the loop. This leads to mode-locking in the F8L.

Erbium in glass has a bandwidth of approximately 40 nm. This means that the shortest pulse obtainable is close to 60 fs. If the spectrum of the pulse envelopes the gain bandwidth of the amplifier, the pulse is said to be transform-limited, meaning that all the frequencies that can be supported by the amplifier are present in the pulse. The time bandwidth product is 0.32 if their envelope is described by 'sech' function. The advantage of using a passively mode-locked laser is that there is no need for an external supply for the modulating element.

The ability of the F8L to produce solitons arises from the fact that the configuration allows pulse compression. As the pulse gets shorter, energy is redistributed along its spectral components leading to higher intensities. It is well known that the balance of negative group velocity dispersion and self phase

modulation are essential for the production of solitons. Glass exhibits negative group velocity dispersion at the wavelength of interest, namely, $1.55 \mu\text{m}$. Since the amplification and pulse compression induced by the NALM lead to very high intensities, with a balance between the dispersion and the self phase modulation, solitons are formed.

FOOTNOTES

- ¹M. E. Fermann, F. Habrel, M. Hofer and H. Hochreiter, *Opt. Lett.* **15**, 752 (1990).
- ²E. Desurvive, J. R. Simpson, P. C. Becker, *Opt. Lett.* **12**, 888 (1987).
- ³P. W. France, *Optical Fiber Lasers and Amplifiers* (CRC Press, Florida, 1991).
- ⁴Kiyoshi Nakagawa, Shigendo Nishi, Kazuo Aida and Etsugo Yoneda, *Journal of Lightwave Tech.*, **9**, 199 (1991).
- ⁵V. J. Mazurczyk and J. L. Zyskind Polarization Hole Burning in Erbium Doped Fiber Amplifiers, Conference on Lasers and Electro-Optics (Baltimore 1993).
- ⁶A. K. Ghatak and K. Thyagarajan *Optical Electronics* (Camebridge University Press, Camebridge, 1989).
- ⁷Walter Koechner *Solid-State Laser Engineering* (Springer-Verlag, Heidelberg, 1976).
- ⁸V. J. Mastas, D. J. Richardson, T. P. Newson and D. N. Payne, *Opt. Lett.* **18**, 358 (1993).

CHAPTER IV

EXPERIMENTAL INVESTIGATIONS

This chapter presents the experiments conducted and the results obtained. First, the characteristics of the Erbium Doped Fiber Amplifier are obtained, and then the construction and results of the Figure Eight Laser built along with the various components used will be discussed.

Characterization of Erbium Doped Fiber Amplifiers

As explained in the earlier chapter the parameters that are necessary to completely characterize an EDFA are the signal absorption coefficient α_s , pump absorption coefficient α_p , and the threshold pump power P_{th} . The procedure for measuring the pump and the signal decay is similar. It consists of measuring the signal (pump) in the fiber along its length, the slope of which will give the required parameter. The procedure for measuring P_{th} , is to inject a known amount of signal power into the fiber and increase the pump until the signal output at the end of the fiber reaches the signal input power level. In the earlier chapter the equations that describe pump and signal behavior in an EDFA, Eqns (3-2a) and (3-2b) can be solved

in terms of P_i or P_{out} as parameter. Solving these equations with P_{out} as parameter we obtain

$$\ln\left[\frac{P_o}{P_{th}} + \frac{1}{2}\alpha_p L + \frac{1}{2}\frac{\alpha_p}{\alpha_s}\frac{\ln 10}{10}G\right] - \frac{1}{2}\frac{\alpha_p}{\alpha_s}\frac{\ln 10}{10}G - \frac{1}{2}\alpha_p L = \ln\left(\frac{P_o}{P_{th}}\right) \quad (4-1)$$

Following the procedure obtaining the procedure similar to that in Chapter II and substituting $G = 0$ in Eqn (4-1), we are treating a case wherein the total gain experienced by the signal as it passes through the amplifier is zero. This follows directly from the discussion in Chapter III. The following relation can be obtained

$$P_{th} = \frac{2P_{out}(e^{\frac{\alpha_p L}{2}} - 1)}{\alpha_p L} \quad (4-2)$$

The advantage of this method is that it is not necessary to know the pump power at the beginning of the fiber precisely. By measuring the pump power at the output end of the fiber, P_{th} can be calculated.

Measurement of Decay Constants

The experimental setup used to measure pump decay constant, α_p and signal decay constant, α_s is shown in Figure 17. A Wavelength Division Multiplexer (WDM) is used to couple 980 nm radiation into the EDFA. The advantage of using the WDM is that the same setup can be used to measure the pump decay, signal decay, and threshold power. The conventional technique for measuring either the pump or signal absorption is the cutback method¹, wherein the pump (signal) is

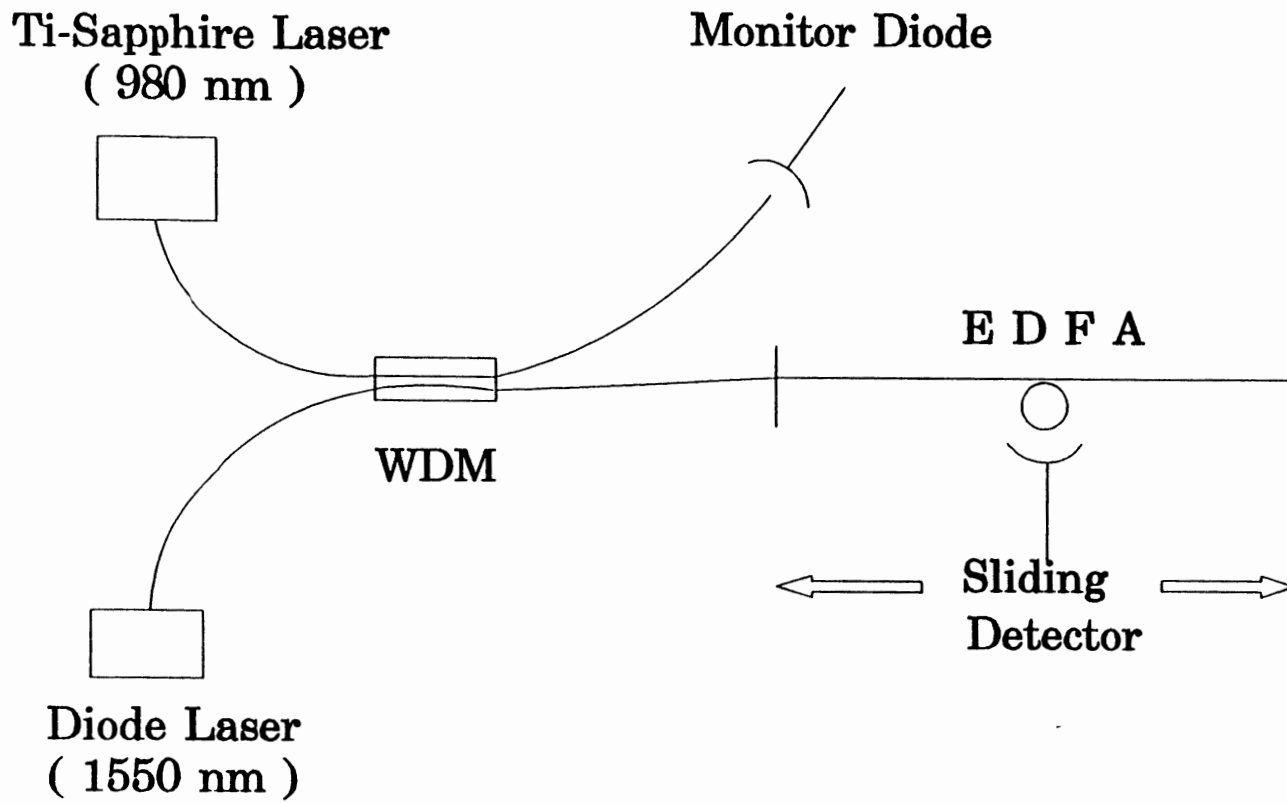


Figure 17. Schematic of the Experimental Setup Used for Measurements

launched into the fiber and the power transmitted by the fiber is measured using a power meter. A specified length of the fiber is then cut and the power emerging out of the fiber end is measured again. It is assumed that all the losses that occur originate from the absorption in the fiber. Knowing the amount of pump absorbed in the specified length of fiber, the decay constant for either pump or signal is calculated. The cutback method is time consuming and destroys the fiber amplifier under study.

To overcome the disadvantages of the cutback method, advantage is taken of the fact that a bent waveguide does not behave like a perfect waveguide and some power is coupled out as radiation modes. Non-invasive signal monitoring, using a macrobend in a standard single mode fiber, has been used in optical systems and in signal processing schemes using tapped delay lines². When a waveguide is bent, the conditions necessary for total internal reflection are not satisfied for all the guided rays, and energy is coupled out as radiation modes. The loss per unit length experienced by a fiber bent to a radius R is

$$\alpha_c = A_c R^{-0.5} e^{-UR} \quad (4-3)$$

where A_c and U are constants for a given fiber³. If the bend radius is kept constant, the amount of power that is coupled out of the waveguide or fiber is a function of the power in the fiber. Since the power radiated from the fiber is a sensitive function of the bend radius, it is extremely important that the bend radius be kept constant. A schematic of the detector used to record the radiated power is shown in Figure 18. Fiber is bent along a glass cylinder of radius 3.5 mm. The glass rod abutting the

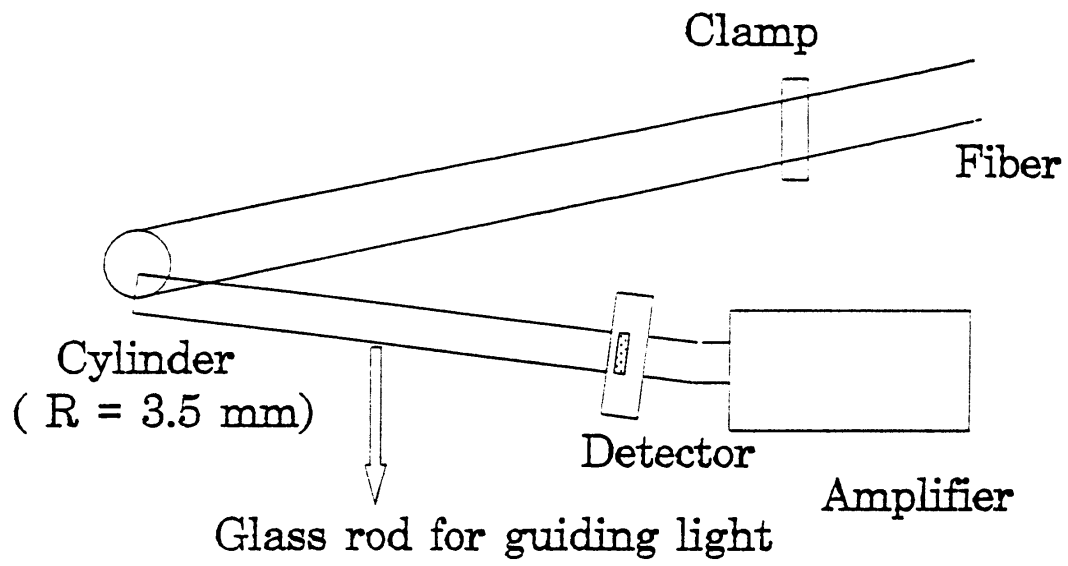


Figure 18. Schematic of the Sliding Detector

cylinder guides a part of the radiated light to the detector. Since it is important that the radius of the bend be constant, a clamp is used to fix the fiber. As the power levels intercepted by the diode placed at the end of the glass rod are very low, an amplifier is used.

To measure pump decay a Ti-Sapphire laser with a single plate birefringent tuning element for wavelength selection, pumped with an Argon-ion laser has been used as the source of 975 nm. The Ti-Sapphire laser produced approximately 0.5 W of power at 975 nm with an Argon-ion laser power of 7 W. The diode laser connected to the other input port of the WDM was deactivated so as not to let any radiation at 1550 nm enter the EDFA. Infrared radiation from the laser is coupled into the fiber using a simple coupling stage. Since the WDM used for the measurement purposes does not have the fourth port to monitor the pump or signal input powers, methods were developed wherein the pump or the signal power at the input of the fiber need not be accurately known. It is important to note here that the power that enters the erbium fiber be less than the threshold power since above the threshold power, the pump decay is not exponential but linear according to Eqn (2-10a). Figure 19 illustrates the pump decay with respect to the normalized fiber coordinate. It is obvious from the illustration that above the threshold power the pump power decay in the fiber is not exponential. As the power in the fiber approaches P_{th} the decay becomes exponential. The output from the Ti-Sapphire laser has been measured to be equal to 5 mW. Assuming that the coupling efficiency is 50%, power in the fiber can be approximated to be 2.5 mW. As mentioned earlier it is not

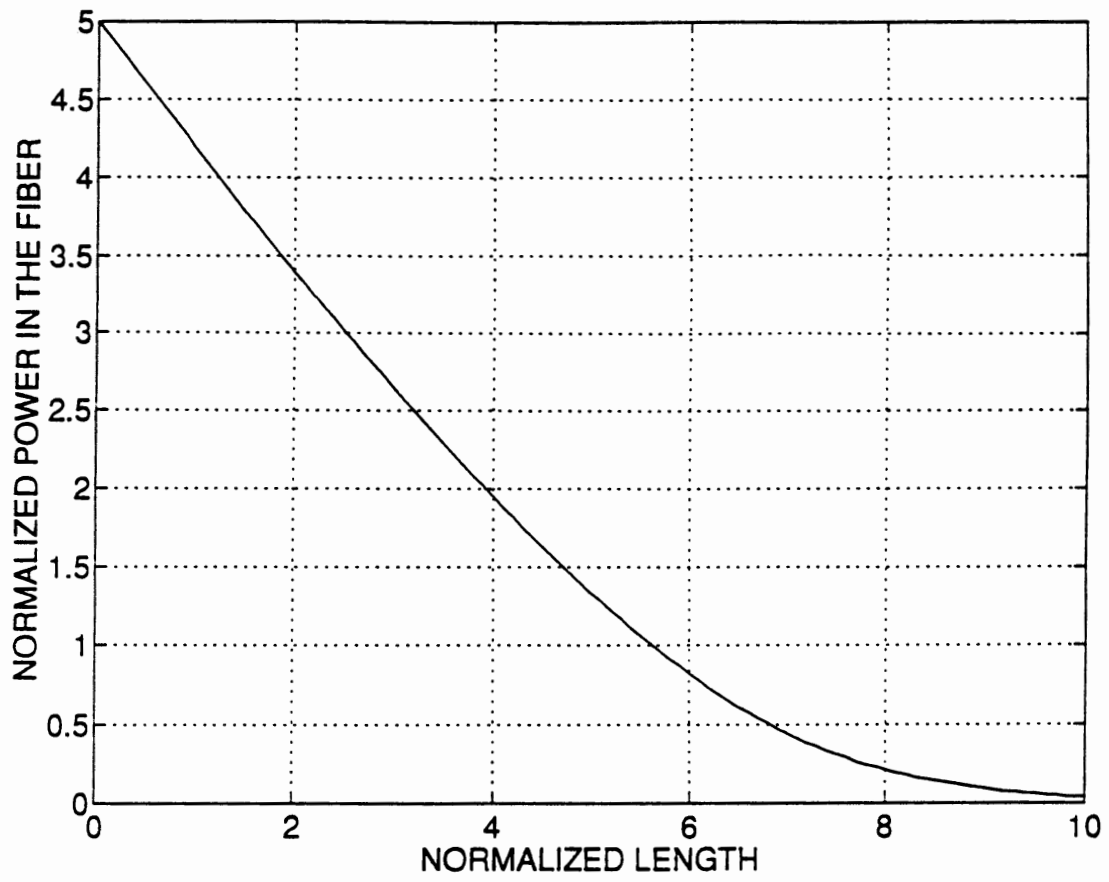


Figure 19. Normalized Length vs Normalized Pump Power

essential that the power in the fiber be precisely known. The length of the fiber used for the measurements was 2.46 m. The fiber is introduced into the detector setup with a Silicon diode at the end of the glass rod. The readings of the detector are recorded as it is moved from the pump end of the fiber. Power is recorded at 25 cm intervals. The readings obtained by the detector are relative, since these suffice for the calculation of the pump decay constant, the disadvantage of not knowing the pump power in the fiber accurately is overcome. A plot of the power recorded by the sliding detector along the length of the fiber is shown in Figure 20. From the graph, the pump decay constant (α_p) has been calculated to be 0.021 cm^{-1} .

The procedure for measuring the signal decay is similar to the one described above. The 980 nm source is blocked and the diode laser is turned on. The rated output of the diode laser is 1 mW at a source current of 44 mA with a threshold current of 20 mA. The wavelength of the diode laser is $1.558 \mu\text{m}$. The source current is fixed at 30 mA to give an output of 0.3 mW. The power entering the Erbium fiber is estimated to be $200 \mu\text{W}$. As in the earlier case the detector is moved along the fiber. The Silicon detector of the earlier case is replaced by a Germanium detector since Silicon has low absorption at wavelengths above 1000 nm. Power in the fiber is recorded at 25 cm intervals. Figure 21 shows the decay of diode signal in the fiber. From the graph, the signal decay constant (α_s) is calculated to be 0.052 cm^{-1} .

Measurement of Threshold Pump Power

As mentioned earlier, the procedure for measuring P_{th} is to take a fixed length

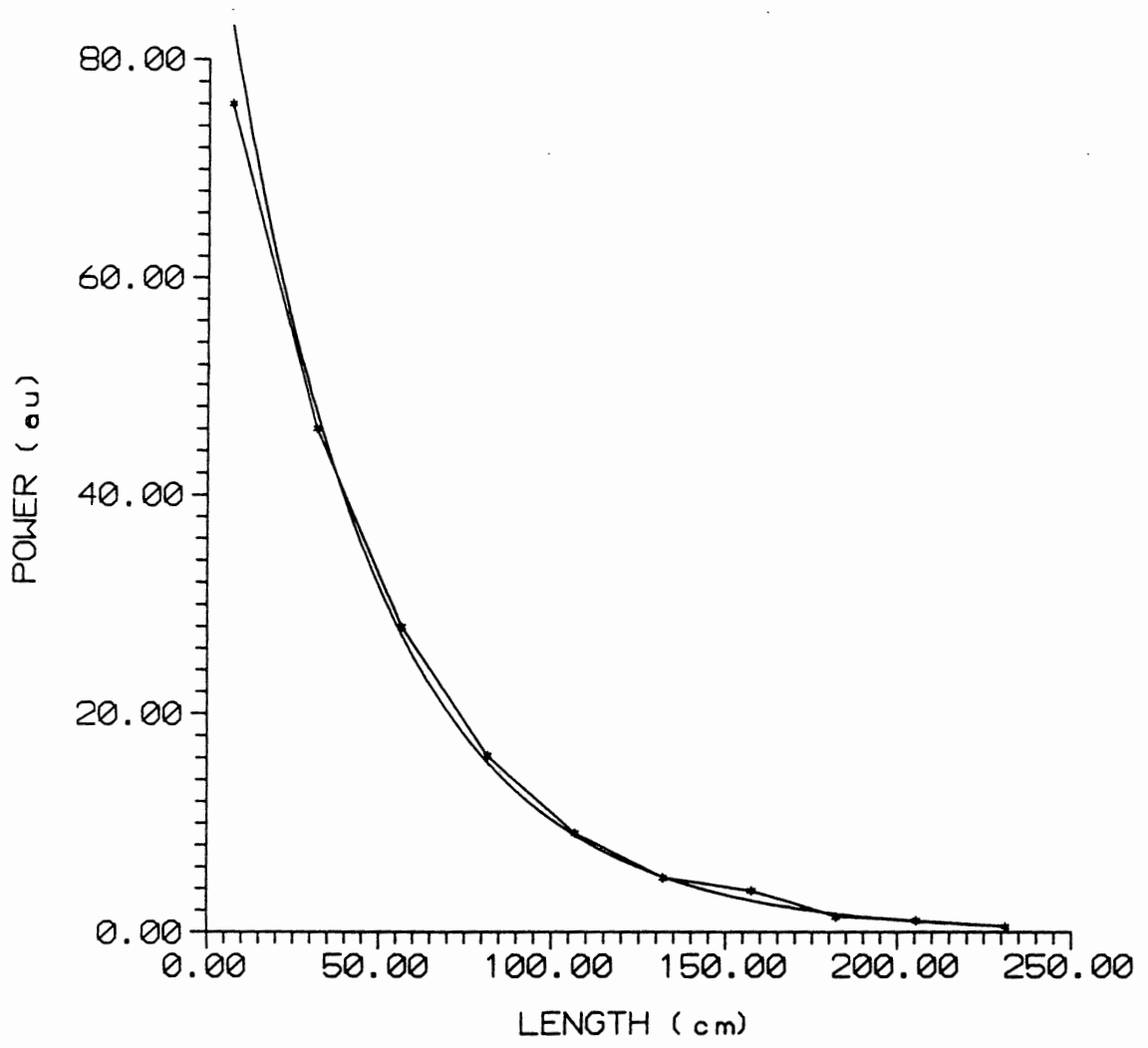


Figure 20. Pump Decay

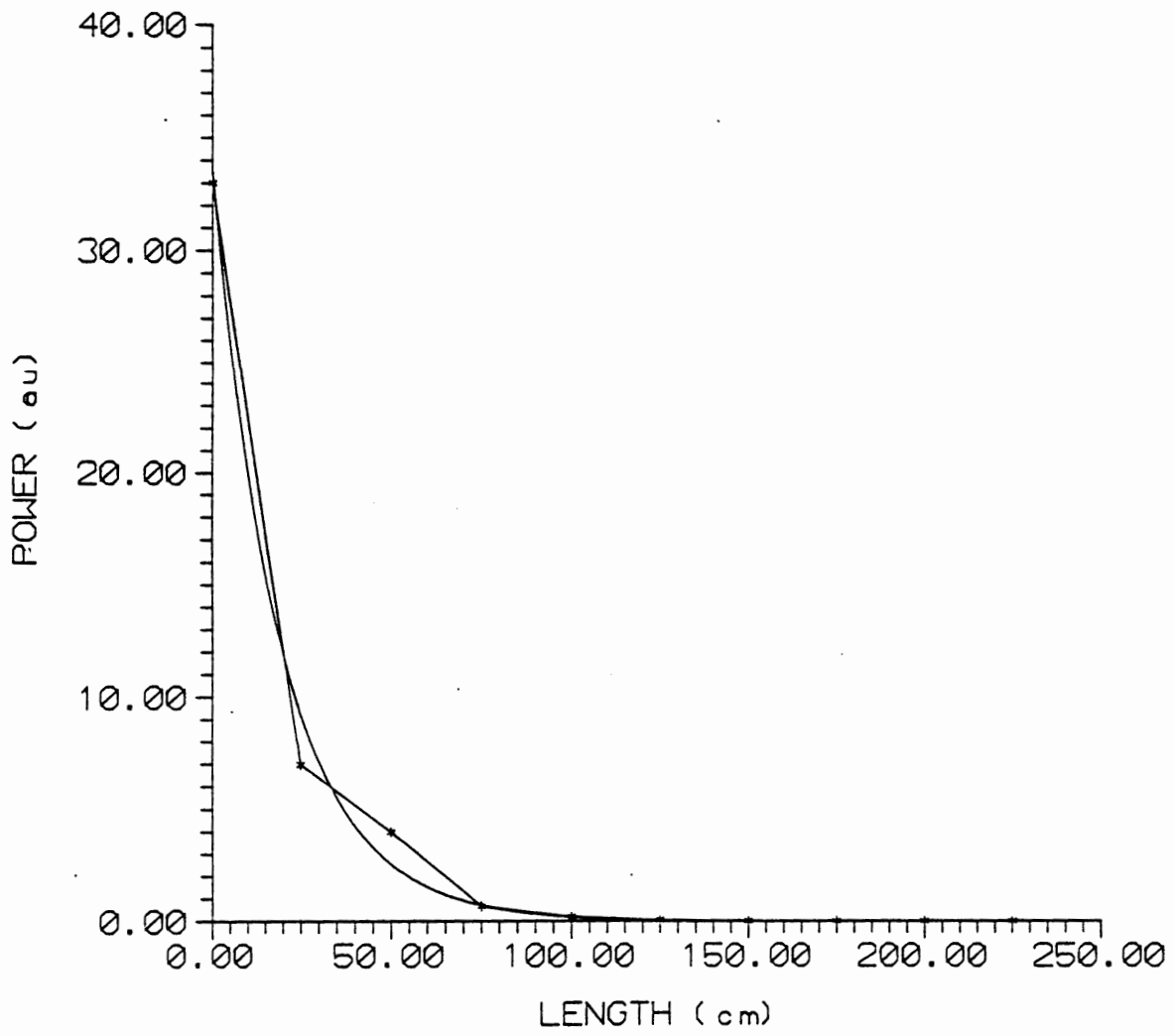


Figure 21. Signal Decay

of fiber and inject both signal and pump into the fiber. Knowing the value of signal power at the beginning of the erbium fiber, the signal power at a fixed distance from the beginning of the fiber is monitored. With no pump power present, the signal is absorbed by the fiber. As the pump power is increased, signal absorption decreases leading to a transparent fiber, and as the pump power is increased further the fiber acts like an amplifier. This is the basic gain dynamics of a three level system. But if we can record the pump power at which a specified length of fiber becomes transparent, using Eqn (4-2) the threshold power can be calculated. The length of the fiber used for the threshold measurement was 2.46 m. The length of fiber under consideration was only 2 m. Signal output of 0.3 mW from the diode laser with a bias current of 30 mA is launched into the WDM. The sliding detector is fixed at the beginning of the fiber and this signal intensity is recorded using a Germanium diode. The sliding detector is moved exactly two meters from the initial point. In the absence of pump power, the signal power recorded by the detector is very low as the signal is absorbed by the Er atoms in the fiber. Now the pump power is increased. As the pump power increases, the signal absorption decreases and a point is reached when the signal intensity recorded by the detector diode is equal to the value recorded at the beginning of the fiber. Schott Glass made filter BG 40 is used to prevent the 980 nm radiation from reaching the Germanium diode. The transmission of the filter is found to be 0.40 at 1550 nm and 0.008 at 980 nm. Now the power at the end of the fiber (2.3 m) is recorded using a power meter. This was found to be 2 mW. Since we understand that the power in the fiber at the point where the net gain is zero

is less than the threshold power, and since we know the pump absorption coefficient, pump power at the point where the fiber is transparent can be calculated using the exponential decay law. Then using Eqn (3-2), the threshold power can be calculated. It has been found that the threshold power is equal to 5.2 mW.

Knowing the three parameters necessary for characterization, the characteristics of the EDFA are simulated. With this the characterization of EDFA is complete and these results are used while making a Figure Eight Laser which will be explained in the next section.

Figure Eight Laser

The aim of this section is to introduce the components used in the fabrication of the Figure Eight Laser, explain their significance and principle of operation and finally look at the Figure Eight laser made and present the results obtained. A schematic of the Figure Eight Laser is shown in Figure 22. To this end the organization of this section is as follows. First the all-fiber polarization controllers are discussed along with the significance of their presence, principle of operation and method of fabrication. Next the isolator used in the auxiliary loop is discussed. Later the operation of the Figure Eight Laser made is discussed.

Polarization Controllers.

In a conventional single mode fiber the polarization of the signal is not

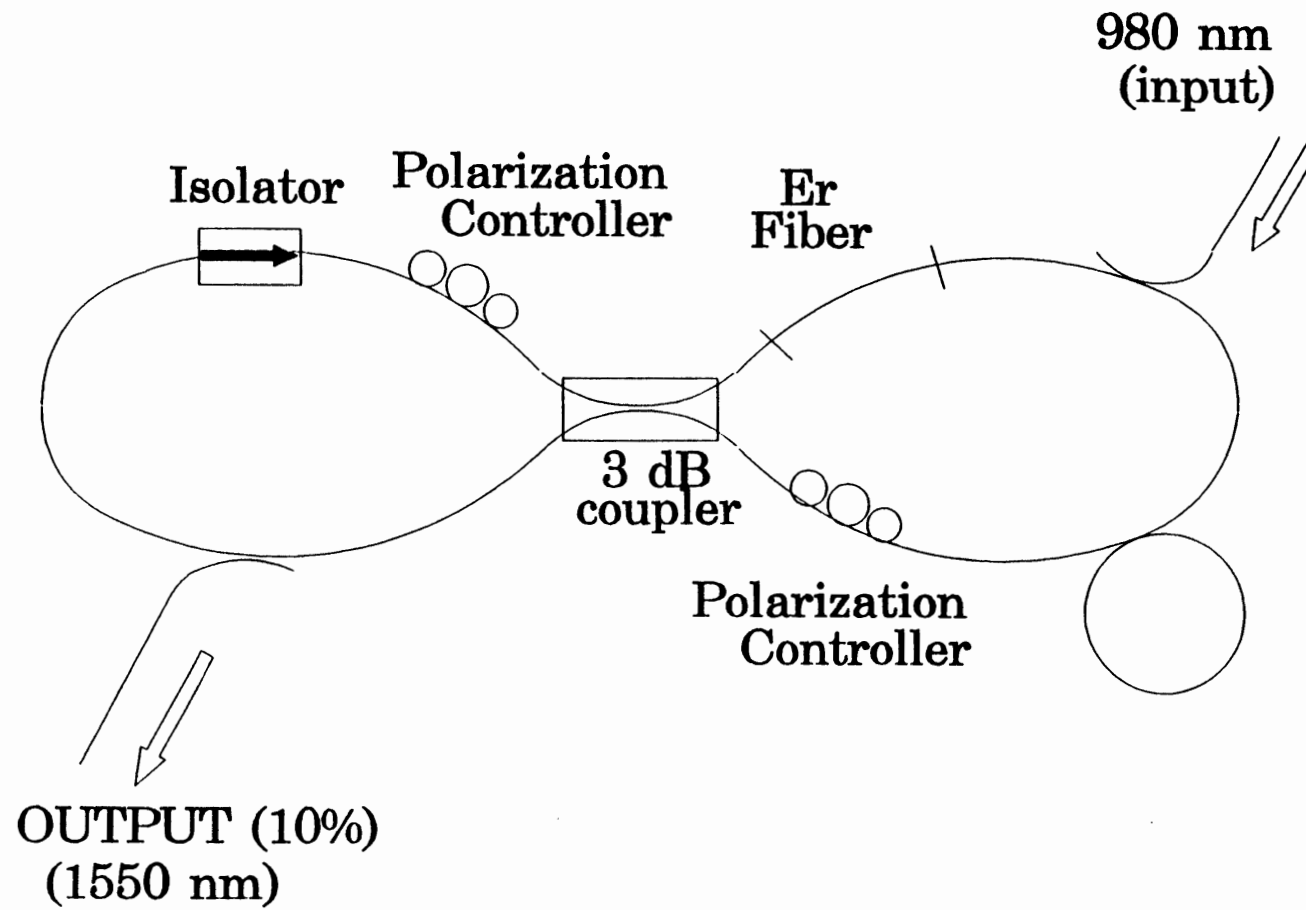


Figure 22. Schematic of the Figure Eight Laser

preserved as it traverses the fiber. A single mode fiber is not truly single mode for it can support two degenerate modes that are dominantly polarized in the two orthogonal directions. Under ideal conditions of perfect cylindrical geometry and isotropic material, a mode excited with its polarization in the x direction would not couple to the mode with orthogonal y polarization state. However, in practice small deformities in the geometry of the fiber and material anisotropy result in the mixing of the two polarizations by breaking the mode degeneracy. Mathematically the mode propagation constant β becomes slightly different for the two modes polarized in the x and y direction. This property is referred to as modal birefringence. The degree of modal birefringence B is defined by

$$B = \frac{|\beta_x - \beta_y|}{k_o} = |n_x - n_y| \quad (4-4)$$

where n_x and n_y are the effective mode indices in the two orthogonal polarization states. As a result of the difference of the propagation constant associated with the two modes, the polarization of the signal transmitted by the fiber reaches an arbitrary state.

There also exists a class of fibers known as polarization preserving fibers, wherein a large amount of birefringence is introduced intentionally so that small random fluctuations will not affect the polarization. The use of polarization preserving fibers requires the identification of slow and fast axis. Since these fibers were not used in making the Figure Eight Laser, further discussion is not entertained. As a conventional single mode fiber is used, the polarization of the signal emerging

from the fiber is arbitrary. The Nonlinear Amplifying Loop is an interferometric device. It is recalled that two orthogonal polarizations do not interfere, hence a device is required which will convert the arbitrary polarization into linearly polarized state. To this end all-fiber polarization controllers are used.

It is well known that when a fiber is bent, stress is induced in the fiber. Applying the theory of elasticity⁴, it has been found that by bending a fiber to a radius R, the difference in the extraordinary and ordinary refractive index produced is

$$\delta n = -a \left(\frac{r}{R} \right)^2 \quad (4-5)$$

where a is the photoelastic constant of the fiber equal to 0.133. This birefringence introduced is small in comparison with the crystal birefringence, but because it is integrated along the fiber the total effect can become significant. In particular, it is possible to coil a fiber with a number of turns N and with a radius R in order to give a total phase delay between the modes of π , $\pi/2$ or $\pi/4$. Thus we have

$$|\delta n| 2\pi N R(m, N) = \frac{\lambda}{m} \quad (4-6)$$

where $m = 2, 4, \text{ or } 8$. Therefore

$$R(m, N) = \frac{2\pi a r^2}{\lambda} N m \quad (4-7)$$

Using the above analysis polarization controllers were made. The radius of the coil was fixed at 16.5 mm. The number of turns used for half-wave and quarter-wave

plates are 4 and 2. It has been shown⁵ that a freedom of coil rotation of $\pm 48.6^\circ$ is sufficient to adjust any polarization.

Isolator

An isolator is the optical analogue of a diode. The isolator plays a very significant role in this configuration. Light that is transmitted by the NALM is unaffected by the isolator whereas light reflected by the NALM is absorbed by the isolator. Thus, it removes unwanted light from the cavity and provides low loss for the high intensity beam and aids in mode-locking the laser.

Functionally an isolator lets light pass through in one direction and prevents its transmission in the other. The famous Faraday effect is used to build a nonreciprocal device like an isolator. Michael Faraday discovered that when a block of glass is subjected to strong magnetic field it becomes optically active. When plane polarized light is sent through glass in a direction parallel to the applied magnetic field, the plane of vibration is rotated. The amount of rotation observed for any given substance is found to be proportional to the field strength B and to the distance light travels in the medium. This rotation can be expressed by the relation

$$\theta = VBL \quad (4-8)$$

where B is the magnetic field, L is the length of the sample, and V is the Verdet Constant. Faraday effect is related to the direct and inverse Zeeman effects. A ferrite is a material that exhibits a large Verdet constant. A good example of a ferrite is an Yttrium-Iron Garnet crystal.

When an electromagnetic wave travels through a ferrite, it produces a magnetic field in the material, at right angles to the direction of propagation. If an axial magnetic field from a permanent magnet is applied, a complex interaction takes place. With only the axial dc magnetic field present, the spin axes of the spinning electrons align themselves along the lines of the magnetic force. Electrons spin because this is a magnetic material. In other materials spin is said to take place also, but each pair of electrons has individual members spinning in opposite directions, so that there is an overall cancellation of the spin momentum. The so called unpaired spin of the electrons in a ferrite causes the individual electrons to have an angular momentum and a magnetic moment along the axis of spin. Each electron behaves like a gyroscope. When a magnetic field due to the propagating field is applied, perpendicular to the axial magnetic field, the electrons precess about the original spin axis. This is due to the gyroscopic effects involved. Because of the precession, a magnetic component at right angles to the two is produced. This has the effect of rotating the plane of the polarization of the waves propagating through the ferrite⁶.

A conventional isolator consists of a ferrite crystal sandwiched between two polarizers with their transmission axes oriented at 45° to one another. Light entering the polarizer is polarized by the first polarizer then rotated by the ferrite and passes through the next polarizer which is oriented at an angle commensurate with the rotation obtainable in the crystal. For a counter propagating beam, the beam is polarized by the oriented polarizer and its plane of polarization is rotated by the ferrite and by the time it reaches the second polarizer its polarization is perpendicular

to the transmission axis of the polarizer and it is absorbed by the polarizer. Thus, a nonreciprocal device is built. In a commercial isolator, two birefringent wedges are used to overcome the polarization dependent loss of the forward transmitting beam. In the present configuration an isolator with 60 dB extinction ratio is used.

Figure Eight Laser

The different components that are used to make the Figure Eight Laser are directional couplers, wavelength division multiplexers, optical isolator and polarization controllers. The directional couplers are used to couple and decouple light from the cavity. The couplers used are fused biconic dichroic couplers. The wavelength division multiplexer is used to couple 980 nm radiation into the EDFA. The total length of the active loop is 39.5 m. It consists of a WDM with a total lead length of 1.39, an erbium amplifier of length 2.46 m, a directional coupler (50 : 50) with a lead length of 2.87 m and a fiber of length 32.7 m (including the polarization controller) has been added to the active loop to facilitate the accumulation of phase shift. All the splices were made using a fusion splicer. The total loss in the active loop excluding the absorption due to the EDFA are expected to be less than 1dB. The total length of the passive loop was 10.2 m. The pump source was an Argon ion pumped Ti-Sapphire Laser. Light was launched into the WDM using conventional coupling stages with a coupling efficiency of approximately 50%. The threshold required to mode-lock the laser was found to be 130 mW. It was also observed that once the laser mode-locked, it was possible to decrease the pump power and still

maintain mode-locking. The traces of the pulses as observed on the scope using a pigtailed diode with a response time of 0.2 ns is shown in Figure 23. The spectrum of the pulses obtained is shown in Figure 24. It is seen that the spectrum is asymmetric. The spike at a wavelength of 1.55 μm indicates the strength of the *cw* component in the output of the laser. A low frequency modulation was also observed in the pulses. This is shown in Figure 25. It was also observed that it was possible to change the frequency of this modulation by the manipulation of polarization controllers in the range of 2 - 5 KHz. The structure of the low frequency modulation is shown in Figure 26. It is seen that the pulses that occur at the fundamental repetition rate of 4.098 MHz formed the structure of this pulse. This is of utmost importance in accounting for the instability of the laser as will be explained in the next chapter.

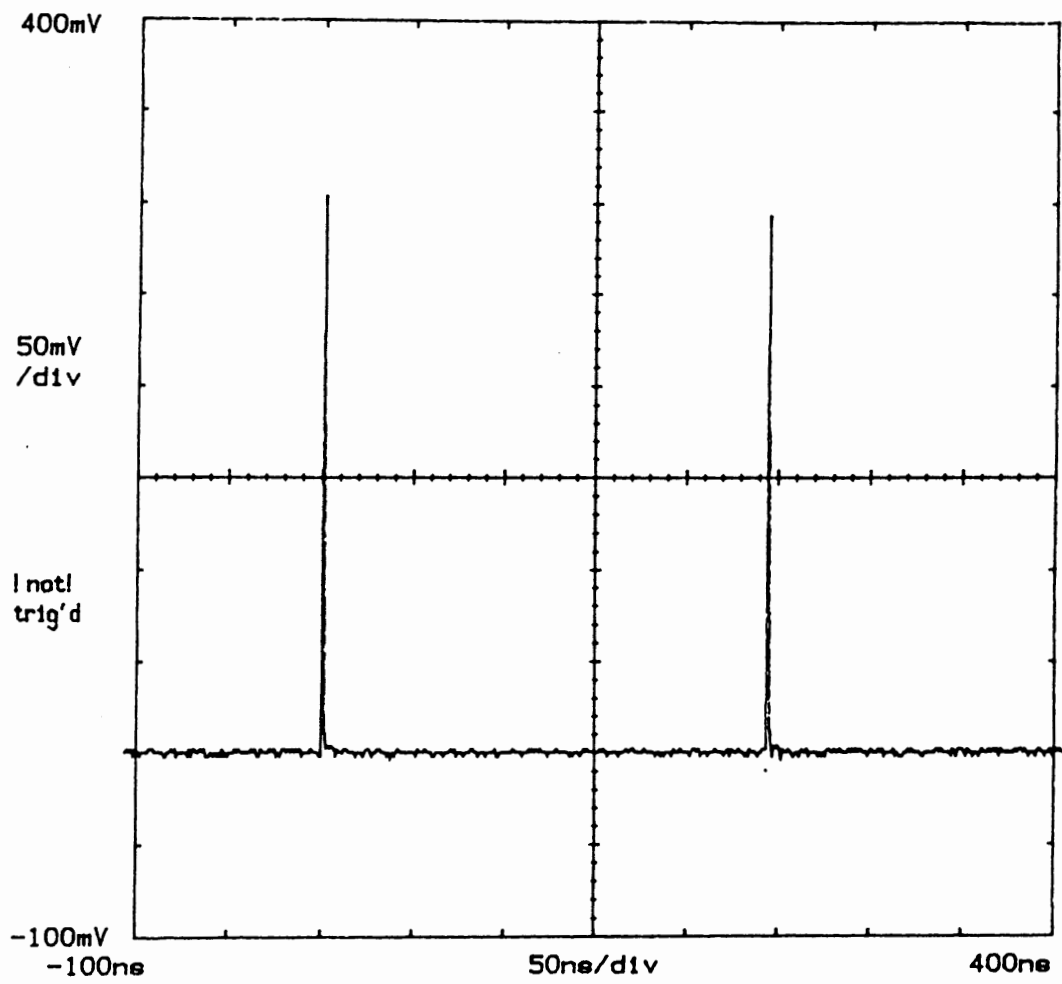


Figure 23. Pulses Recorded by the Detector

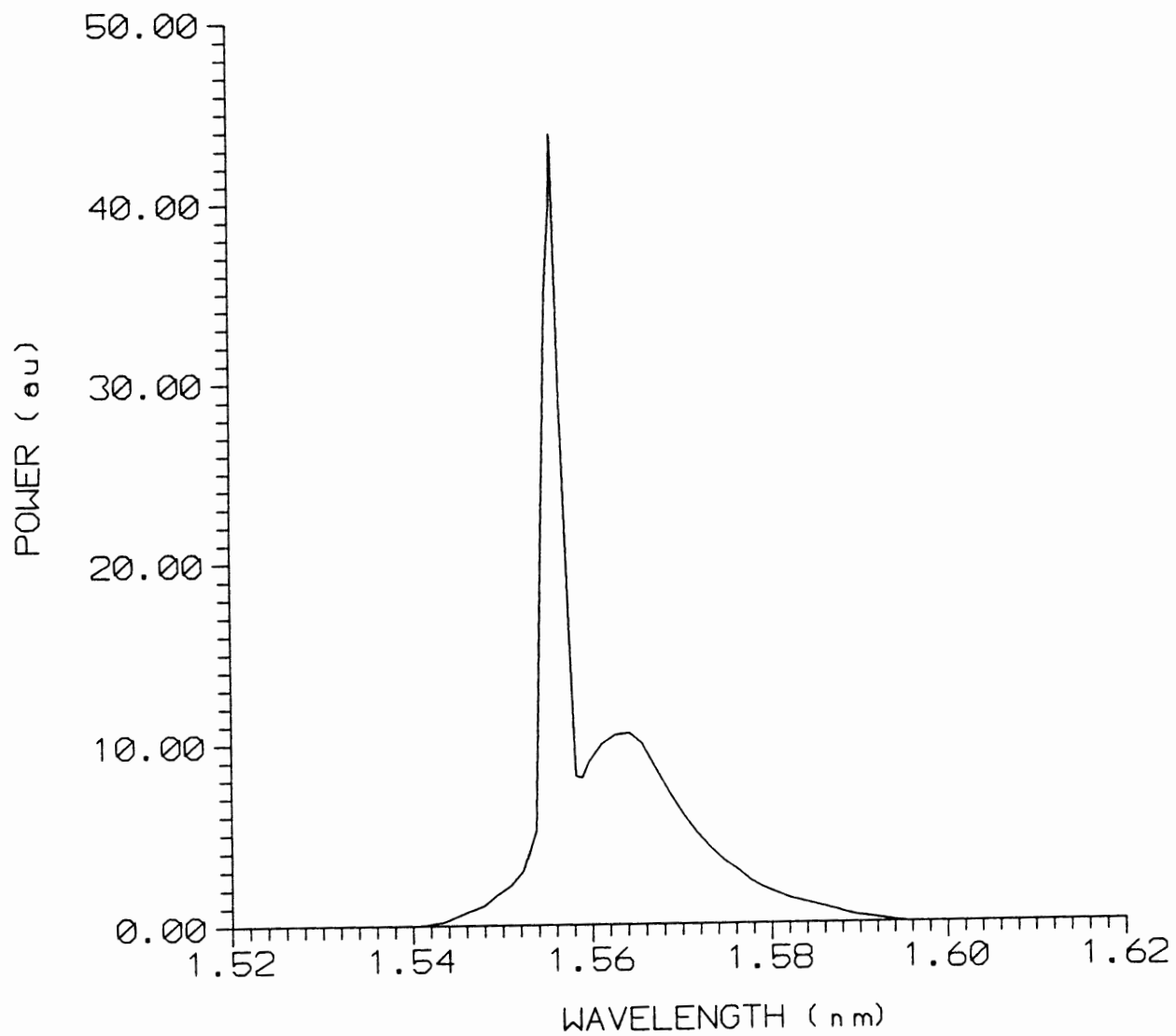


Figure 24. Spectrum of the Pulses

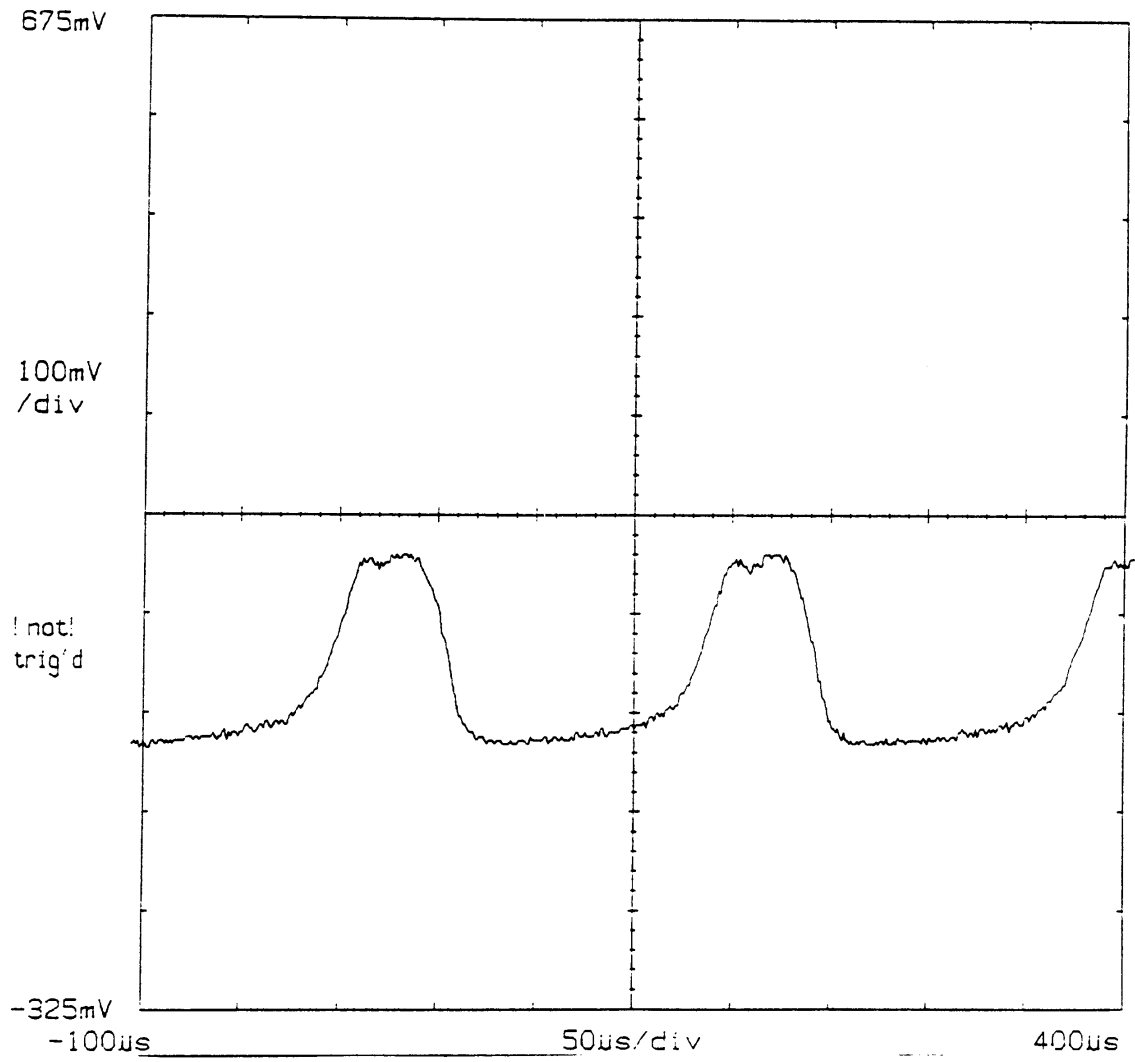


Figure 25. Low Frequency Modulation

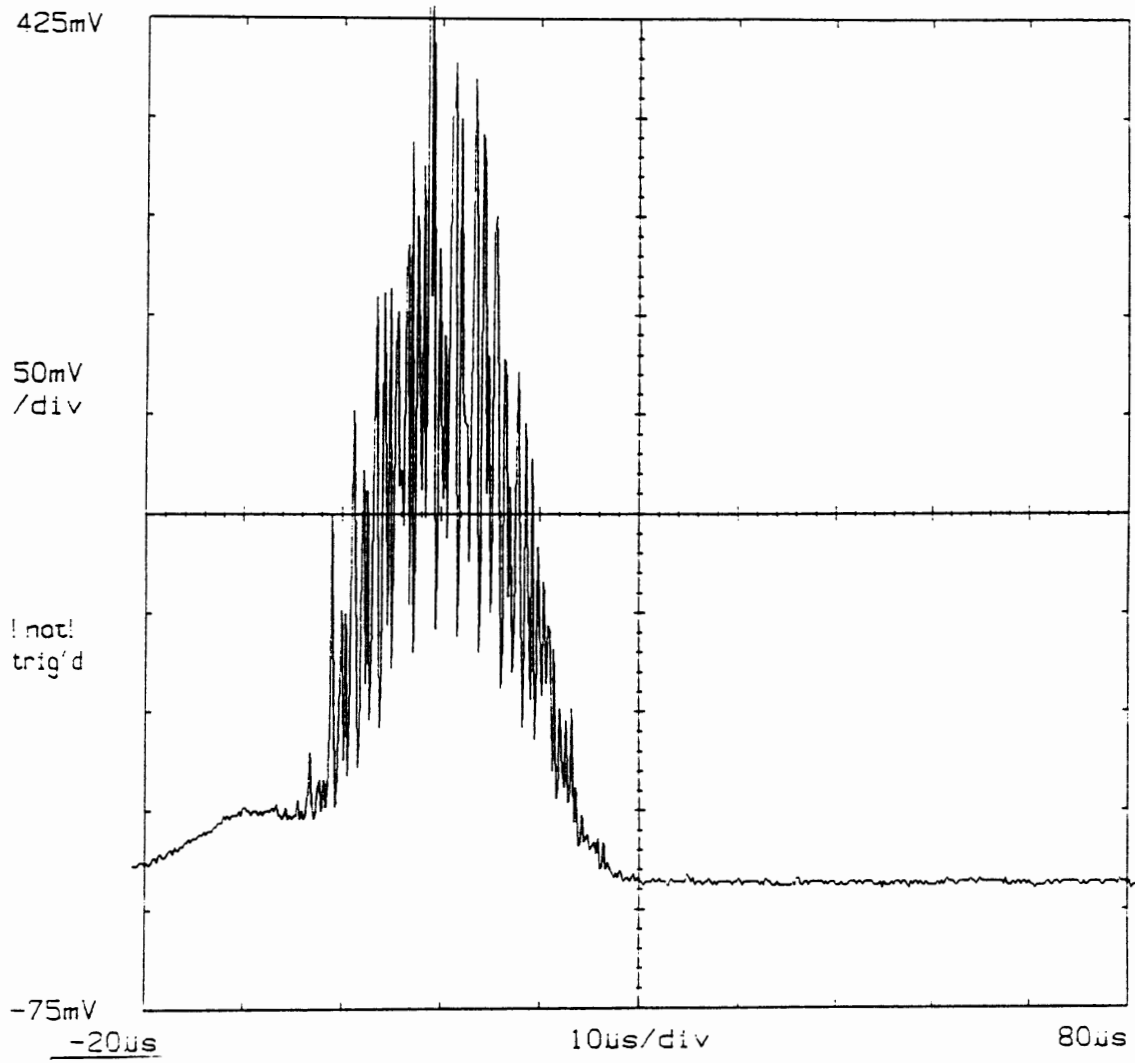


Figure 26. Structure of Low Frequency Modulation

FOOTNOTES

¹DiGiovanni, Single-mode Optical Fiber Measurements: Characterization and Sensing, (Artech House, Boston, 1993).

²J. D. Evankow and R. M. Jopson, IEEE Trans Phot. Tech. Lett. 3, 993 (1991).

³Luc B. Jeunhomme, Single mode Fibers, (Marcel Dekker, New York, 1990).

⁴R. Ulrich, S. C. Rashleigh and W. Eickhoff, Opt. Lett. 5, 273 (1980).

⁵H. C. Lefevre, Elect. Lett., 16, 778 (1980).

⁶George Kennedy, Communication Systems, (McGraw Hill, New Delhi, 1985) Chapter 10.

CHAPTER V

INSTABILITY

It has been speculated earlier¹ that the polarization dependent switching of the Nonlinear Amplifying Loop Mirror is the cause of instability in the Figure Eight Laser. It is the aim of this section to show that the root of instability lies in the gain modulation of the Erbium Doped Fiber Amplifier.

To illustrate the source of instability, consider a Figure Eight Laser with the following parameters. Let the repetition rate of the laser be 4 MHz. This corresponds to a time separation of 250 ns. Let the ratio of the length of the active loop (loop incorporating EDFA) to the passive loop (loop incorporating isolator) be 4 to 1. The pulse width is assumed to be very small. Let us observe the arrival of pulses at the EDFA. As shown in Figure 27, let the clockwise propagating pulse arrive at the EDFA at $t = 0$. After a time lapse of 200 ns the counter propagating pulse arrives at the EDFA after traversing the length of the active loop. Switching occurs and the transmitted pulse after travelling through the passive loop is split by the directional coupler into clockwise and counter-clockwise propagating pulses. After being split by the directional coupler, the first pulse that arrives at the amplifier is the clockwise propagating pulse. The time taken for the switched pulse to traverse

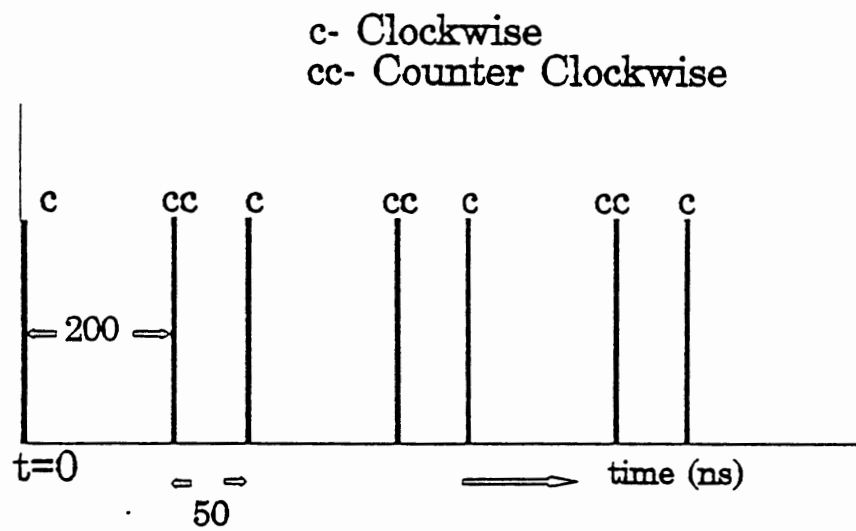


Figure 27. Timing Diagram

the passive loop and to re-enter the EDFA is 50 ns. The time sequence of arrival of pulses shows that 200 ns after the clockwise propagating pulse is amplified the counter-clockwise propagating pulse enters the gain medium. And 50 ns after the departure of the counter clockwise propagating pulse, the clockwise propagating pulse re-enters the EDFA. This means that the time allowed for recuperation of the EDFA is 50 ns for the clockwise propagating pulse whereas it is 200 ns for the counter clockwise propagating pulse. This suggests that the gain experienced by the counter clockwise propagating pulses will be different. It is also seen that the pulse which accumulates phase shift (clockwise propagating) experiences less gain than the counter clockwise propagating pulse. The effect of this is the following. The pulses interfering are of different intensity hence the switching contrast suffers as explained before. It has also been recorded earlier that modulation is observed in the mode-locked train at low frequencies. The reason for the occurrence of this low frequency modulation is the explained as follows.

At $t = 0$, when the laser is switched ON the population difference between the lower and the upper lasing level increases, but as the time for recovery of the EDFA between the occurrence of two pulses is low, the gain medium continues to amplify only as long as the signal experiencing gain is low. With time the signal intensity grows and the population difference decreases to a level where it can no longer maintain the threshold required to maintain mode-locking but high enough for the maintenance of *cw* lasing. So the laser is no longer mode-locked and the output is *cw*. With no pulses present the amplifier recovers to a level where it can resume

mode-locking and this process repeats itself. This presence of the spike in the spectrum of the laser shown in Figure 24 which shows the strength of the *cw* component in the laser reinforces this argument.

Another way of looking at the instability is that there are two switching elements in the F8L cavity. One is the NALM itself and the other is the gain modulation of the EDFA due to the asymmetry of the two loop lengths. This introduces harmonics of the round trip frequency in the F8L. These harmonics permit the growth of additional pulses in the cavity. This means that in addition to just one pulse circulating in the cavity, it should be possible for 2 equally spaced pulses to circulate in the cavity as well as 3 equally spaced pulses. These harmonics would then draw energy from the single intense pulse circulating in the cavity. Eventually, when enough pulses are circulating in the cavity, mode-locking will halt until a single mode-locked pulse can rebuild in strength.

Hence the root cause of modulation in the output of the Figure Eight Laser is lack of enough recovery time for the EDFA, to provide enough gain for the pulse train i.e., lack of symmetry in the time domain.

Since the time difference between the occurrence of the clockwise and counter-clockwise propagating pulse is small, the remedy would be to increase the time separation between the two pulses. To achieve this a long length of fiber is added to the passive loop of fiber so as to give enough time for the EDFA to recover. This is done by balancing the length of the fiber in the active and passive loop.

In the Figure Eight Laser that was made, the length of the active loop was

39.2 m and the length of the passive loop was 10.5 m, making the total length of the loop 49.7 m leading to a fundamental repetition rate of 4.1 MHz. To compensate the length, 29 m of fiber is added to the passive loop, making the total length of the laser cavity equal to 77.7 m. The repetition rate of the laser was 2.646 MHz. A schematic of the modified configuration is shown in Figure 28. The pulse spectrum of the stabilized system is shown in Figure 29. It is seen that the energy of the pulses is now evenly distributed. This shows that there is no concentration of energy in the 1550 nm band. This means that the energy is distributed among the gain bandwidth of the EDFA. It should be recalled (Chapter V) that before the modifications were made, the energy was concentrated in the 1550 nm band, which represents the strength of the *cw* component in the output. In the time domain the pulses did not exhibit low frequency modulation. This confirms the observations made in the frequency spectrum wherein the *cw* component of the laser has been eliminated. The total change in the intensity of the pulses was less than 5 percent. This to our knowledge is the first time that the output of the Figure Eight Laser has been stabilized. The pulses as observed on a sampling oscilloscope are shown on Figure 30. The peak power of the output pulses was measured to be 12 W. The pulse width was estimated to be 290 fs. The time bandwidth product of the pulses was calculated to be 0.36 showing that the pulses were close to being transform-limited. The autocorrelation trace is shown in Figure 31.

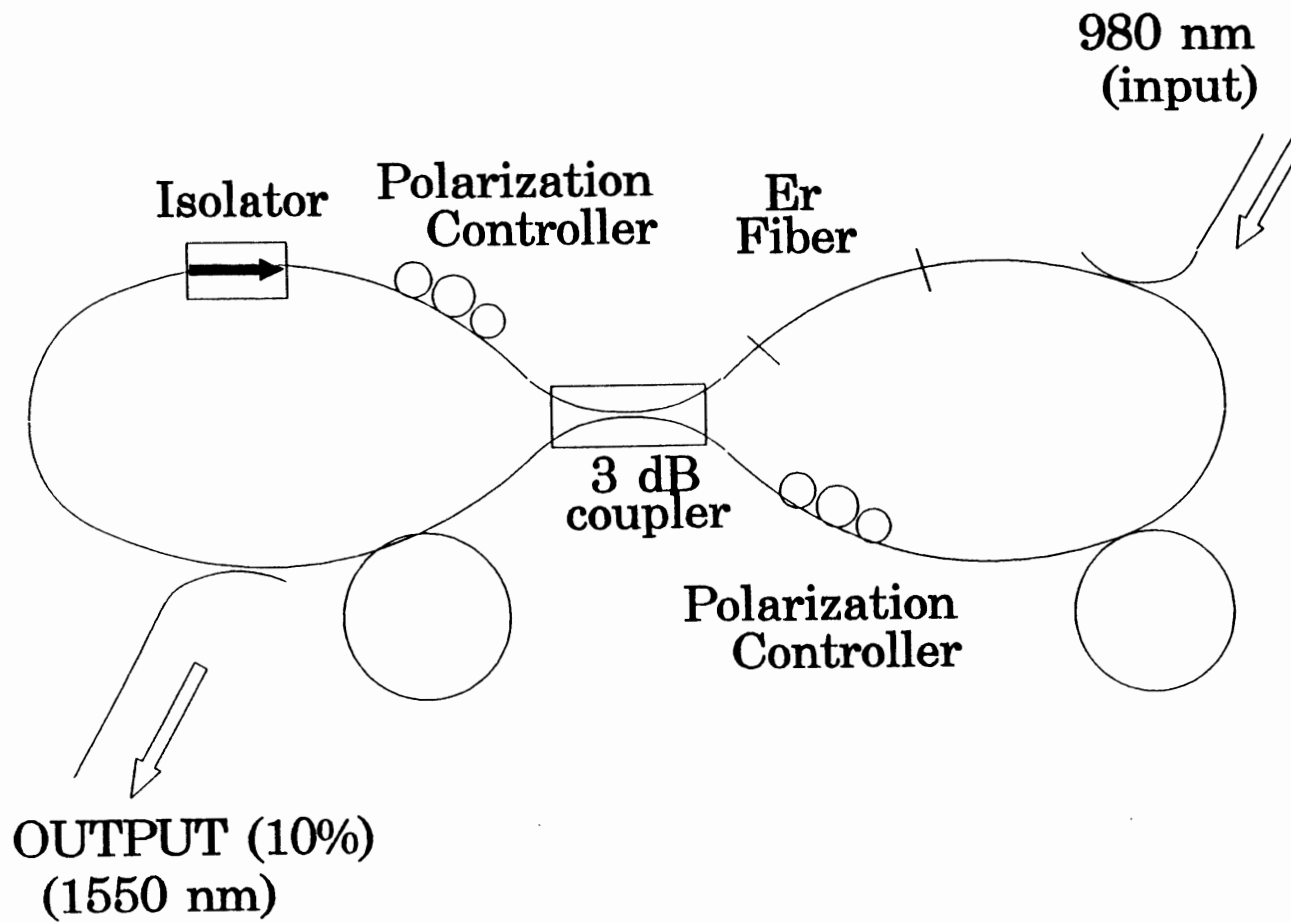


Figure 28. Schematic of the Modified Figure Eight Laser

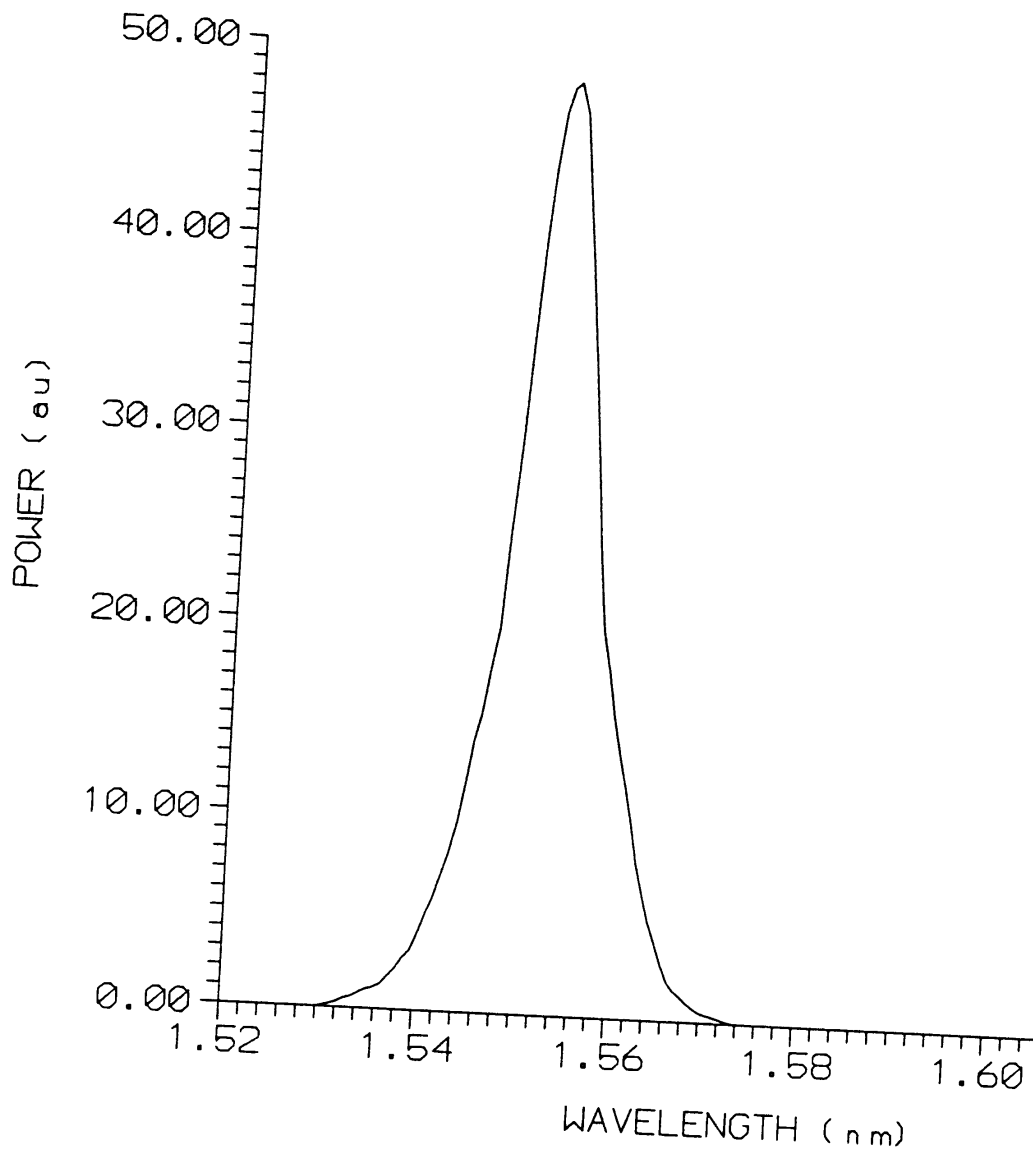


Figure 29. Spectrum of the Pulses

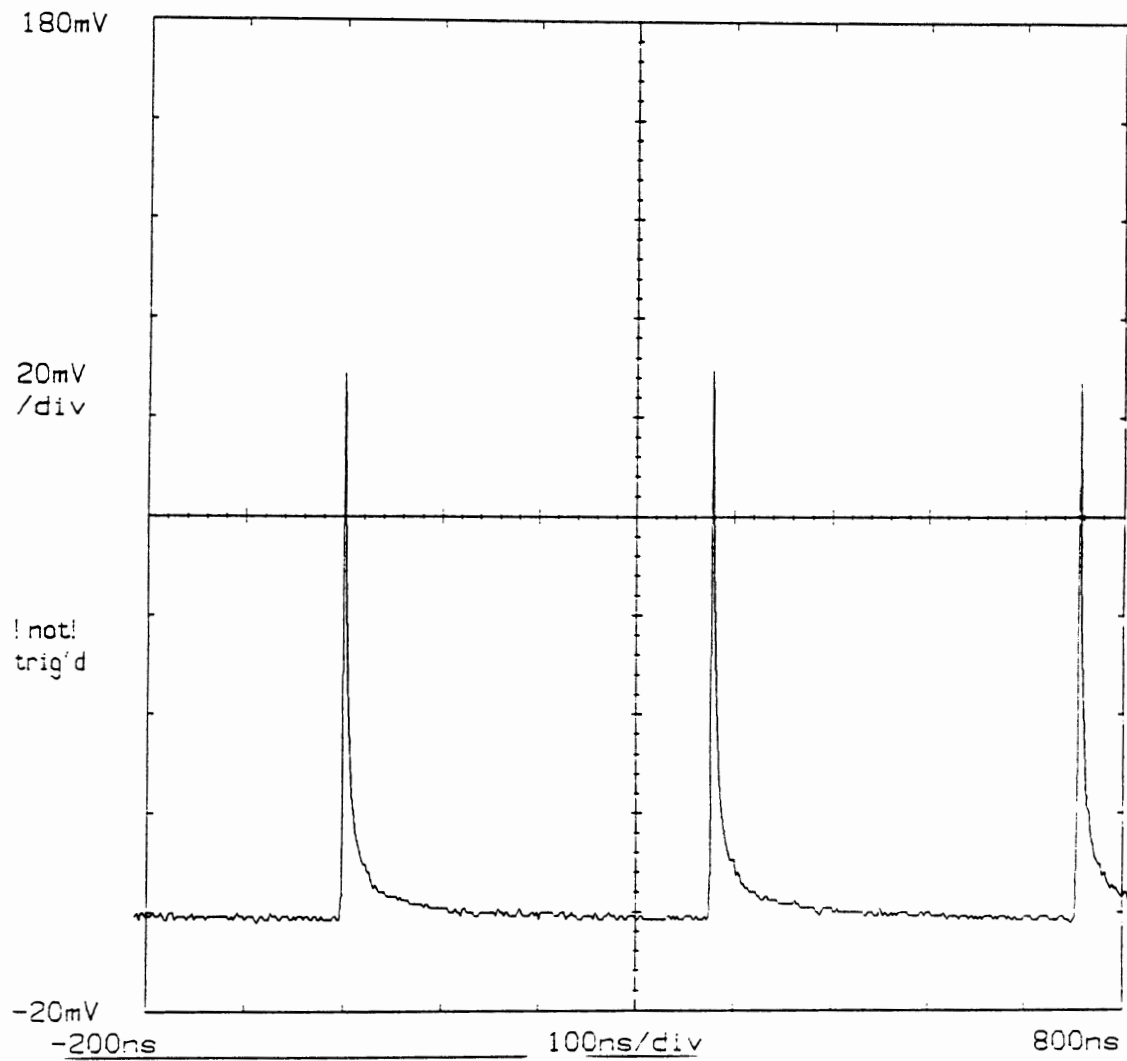


Figure 30. Pulses Recorded by the Detector

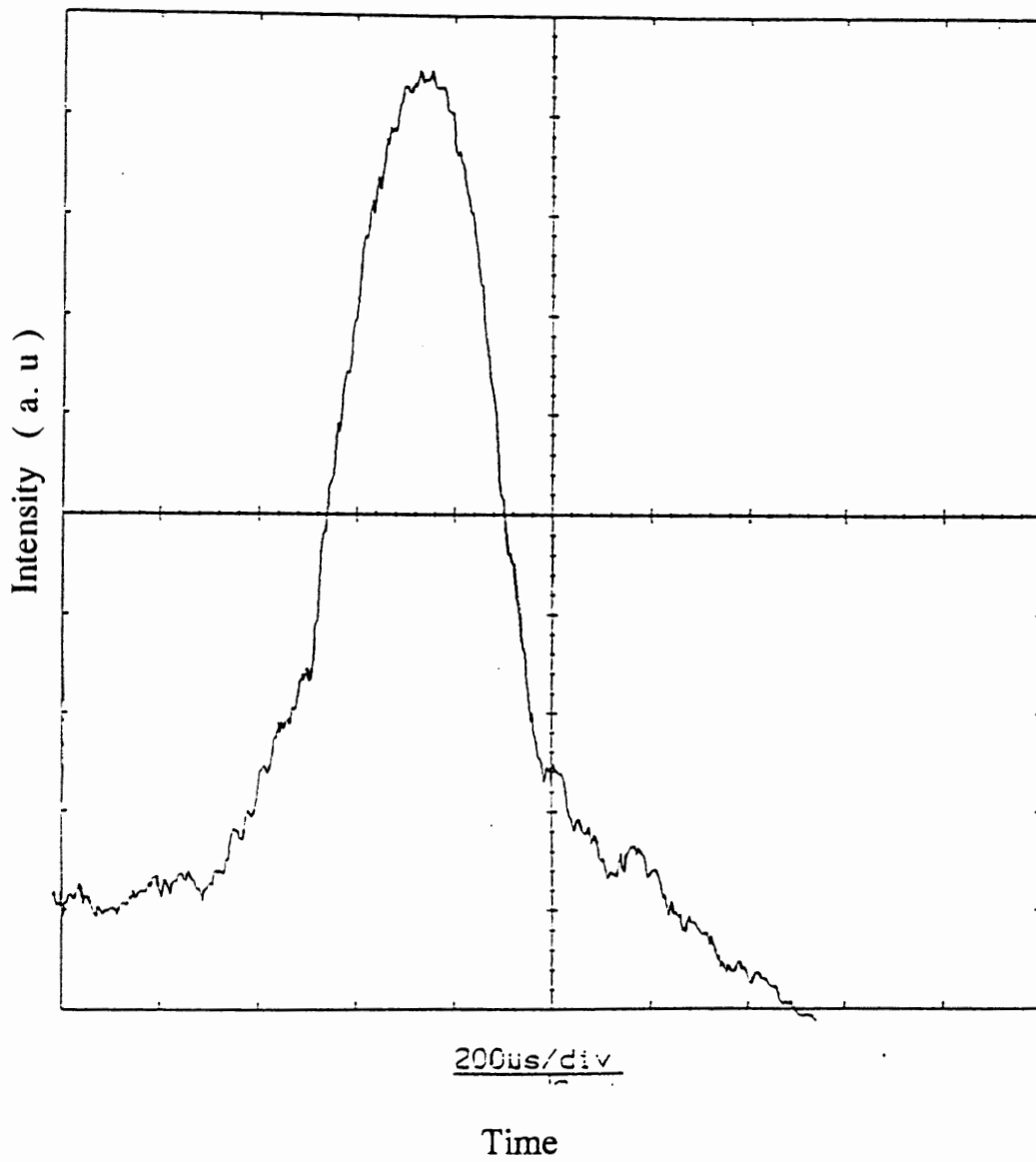


Figure 31. Autocorrelation of the Output Pulses

FOOTNOTES

¹N. Finlayson, B. K. Nayar and N. J. Doran, *Opt. Lett.* 17, 112 (1992).

CHAPTER IV

SUMMARY AND CONCLUSIONS

In this investigation we have presented the ideas and the device configurations that have lead to the development of a stable Figure Eight Laser. We have also presented the origin of the instability and we also have, with proper design improvements, developed the stable Figure Eight Laser. To our knowledge this is the first time that the origin of the instability of the laser has been understood.

In Chapter II, a theoretical investigation into the components and device configurations involved in the development of the Figure Eight Laser have been presented. The analysis of the Erbium Doped Fiber Amplifier has lead to a practical algorithm for the design of an amplifier that can be used in a communication system.

Chapter III presented the experimental investigations conducted and the results obtained, along with the conclusion that have been drawn from the observations. Chapter IV presented the origin of instability in the laser and also suggested and proved the methods of improvements. The importance of the fact that the Figure Eight Laser has been stabilized is that it will lead to further development of systems based on the Figure Eight Laser.

In the end I cannot but pay tribute to Ayn Rand, who had averred, "Nature to

be commanded, must be respected." I could not have found a more perfect example to prove the veracity of this statement. As mankind and technology continue to surge forward, we hope that this small contribution of ours will be trampled upon by posterity to build a new and a better world.

2
VITA

Dasika V. V. Prasad

Candidate for the Degree of

Master of Science

Thesis: STABILIZED MODE-LOCKING OF THE FIGURE EIGHT LASER

Major Field: Electrical Engineering

Biographical:

Personal Data: Born in Khammam, Andhra Pradesh, India, October 20, 1970, son of Dasika Bhaskara Rao and Dasika Radha.

Education: Graduated from Little Flower Junior College, Hyderabad, India, in May, 1987; received Bachelor of Engineering in Electronics Engineering from Sir M. Visvesvaraya Institute of Technology, Bangalore, India, in August, 1991; completed requirements for the Master of Science degree at Oklahoma State University in December, 1993.

Professional Experience: Graduate Research Assistant, Department of Electrical Engineering, Oklahoma State University, 1992-present.